

Geochemical Response of the Mid-Depth Northeast Atlantic Ocean to Freshwater Input During Heinrich Events 1 to 4

Anya J. Crocker^{1,2*}, Thomas B. Chalk^{1,3}, Ian Bailey^{1,4}, Megan R. Spencer¹, Marcus Gutjahr^{1,5}, Gavin L. Foster¹, Paul A. Wilson¹

¹National Oceanography Centre Southampton, University of Southampton, Waterfront Campus, European Way, Southampton SO14 3ZH, UK

²Department of Animal and Plant Science, University of Sheffield, Western Bank, Sheffield, S10 2TN, UK

³Department of Physical Oceanography, Woods Hole Oceanographic Institution, Woods Hole, Massachusetts, USA

⁴Now at: Camborne School of Mines & Environment and Sustainability Institute, College of Engineering, Mathematics & Physical Sciences, University of Exeter, Penryn Campus, Treliever Road, Penryn Cornwall, TR10 9FE, UK

⁵Now at: GEOMAR Helmholtz Centre for Ocean Research Kiel, Wischofstraße 1 – 3, 24148 Kiel, Germany

*Corresponding author

Correspondence to: Anya J. Crocker, anya.crocker@noc.soton.ac.uk

Heinrich events are intervals of rapid iceberg-sourced freshwater release to the high latitude North Atlantic Ocean that punctuate late Pleistocene glacials. Delivery of fresh water to the main North Atlantic sites of deep water formation during Heinrich events may result in major disruption to the Atlantic Meridional

Overturning Circulation (AMOC), however, the simple concept of an AMOC shutdown in response to each freshwater input has recently been shown to be overly simplistic. Here we present a new multi-proxy dataset spanning the last 41,000 years that resolves four Heinrich events at a classic mid-depth North Atlantic drill site, employing four independent geochemical tracers of water mass properties: boron/calcium, carbon and oxygen isotopes in foraminiferal calcite and neodymium isotopes in multiple substrates. We also report rare earth element distributions to investigate the fidelity by which neodymium isotopes record changes in water mass distribution in the northeast North Atlantic. Our data reveal distinct geochemical signatures for each Heinrich event, suggesting that the sites of fresh water delivery and/or rates of input played at least as important a role as the stage of the glacial cycle in which the fresh water was released. At no time during the last 41 kyr was the mid-depth northeast North Atlantic dominantly ventilated by southern-sourced water. Instead, we document persistent ventilation by Glacial North Atlantic Intermediate Water (GNAIW), albeit with variable properties signifying changes in supply from multiple contributing northern sources.

Keywords: Heinrich events; North Atlantic palaeoceanography; Last glacial period; Neodymium isotopes; B/Ca; Carbon and oxygen isotopes; Ice-rafted debris; ODP Site 980.

1. Introduction

The climate of the last glacial period was punctuated by a number of pronounced events with near global impacts, known as Heinrich (or H-) events (e.g. Heinrich, 1988; Hemming, 2004). During these events, transient catastrophic collapses of the North American Laurentide Ice Sheet (LIS), centered over the Canadian Hudson Bay, produced armadas of icebergs that travelled through the Hudson Strait into the North Atlantic Ocean, eventually depositing large volumes of ice-rafted debris (IRD), including distinctive detrital limestone clasts, in a belt across the North Atlantic (Ruddiman, 1977). LIS surging, together with iceberg calving from other circum-North Atlantic and Arctic ice sheets during H-events added large volumes of fresh (low density) water to the (sub)polar oceans with important implications for northern-sourced deep water formation and the Atlantic Meridional Overturning Circulation (AMOC). The AMOC exerts a strong control on regional and global climate on orbital to suborbital timescales, influencing latitudinal heat budgets (e.g. Boyle and Keigwin, 1987; Broecker and Denton, 1989) and partitioning of carbon between the atmosphere and deep ocean (e.g. Adkins, 2013; Sigman and Boyle, 2000; Sigman et al., 2010). Understanding the response of AMOC to fresh water addition is therefore crucial, particularly in light of recently accelerating mass loss from the Greenland Ice Sheet and other circum-Atlantic ice masses (Gierz et al., 2015; Vaughan et al., 2013).

Previously, it was suggested that fresh water inputs at high latitudes during H-events caused a cessation of deepwater formation in the North Atlantic, resulting in a shoaling of the northern component water overturning cell by ~1 km (e.g. Alley et al., 1999; Sarnthein et al., 1994; Swingedouw et al., 2009). Support for this concept of a near complete shutdown of AMOC during H-events came from two main lines of evidence: (i)

a dramatic drop in circulation vigour (e.g. McCave et al., 1995a; McManus et al., 2004) and (ii) water mass provenance reconstructions (including those based on $\delta^{13}\text{C}$, Cd/Ca and ^{14}C) indicating an increased presence of nutrient-rich southern-source waters (SSW) below $\sim 2 - 2.5$ km depth in the North Atlantic Ocean (e.g. Keigwin et al., 1991; Robinson et al., 2005; Stern and Lisiecki, 2013; Vidal et al., 1997). More recently, however, both of these arguments have been questioned. $^{231}\text{Pa}/^{230}\text{Th}_{\text{xs}}$ records from sites across a wide range of water depths suggest that overturning persisted at shallower depths during H1 (Bradt Miller et al., 2014; Gherardi et al., 2009; Lippold et al., 2016), with values compatible with a near complete shutdown only identified in the SSW cell and during H-events close to glacial maxima (Böhm et al., 2015; Lippold et al., 2009; McManus et al., 2004). A further recent development is the documentation of a poorly ventilated water mass in the Nordic Seas during the last glacial period that overflowed the Greenland-Scotland Ridge (GSR) into the Atlantic basin during the deglaciation (Thornalley et al., 2015). This discovery means that the presence of nutrient-rich waters in the North Atlantic basin may no longer be simply attributed to the incursion of waters from the south. Indeed, excursions to low oxygen and sometimes also low carbon isotopic signatures of benthic foraminifera in the North Atlantic during H-events have been interpreted to suggest that there may also have been overflow of waters from the Nordic Seas at these times (e.g. Meland et al., 2008; Thornalley et al., 2010; Vidal et al., 1998). In addition, bulk sediment leachate ϵ_{Nd} values from the northeast North Atlantic (Crockett et al., 2011) are argued to support a persistent presence of overflow waters from the Nordic Seas in the North Atlantic throughout most, if not all, of the last glacial cycle, providing a northern source of nutrient-rich waters to the northeast Atlantic Ocean.

Detailed palaeoceanographic reconstructions show that the classic concept of a simple repeated response of AMOC to freshwater addition during each H-event may be overly simplistic. Not all H-events show a clear perturbation in every oceanographic reconstruction, and there is no consensus on which H-events involve the largest disruption of the ocean-atmosphere system. There is also little agreement about the factors that control the amplitude of AMOC response to freshwater input and considerable debate over the importance of H-event timing relative to the last glacial cycle (Böhm et al., 2015; Lynch-Stieglitz et al., 2014). New high-resolution data sets spanning multiple H-events are therefore needed to help us to gain a better understanding of the range of associated circulation changes in the Atlantic. Records from sites proximal to the GSR are particularly valuable because this region is especially sensitive to changes in northern deep water formation and therefore can help to better constrain variations in the influence of Nordic Seas overflow waters (NSOW).

Bulk sediment leachate Nd isotope data from northeast Atlantic Ocean Drilling Program (ODP) Site 980 (55°29.1'N, 14°42.1'W; 2170 m water depth; location shown in Fig. 1) have been interpreted to suggest that overflow waters crossing the Wyville-Thomson Ridge (WTR) from the Nordic Seas were supplied to the Feni Basin at intermediate depths for much of the past 41 kyr (Crocket et al., 2011), with either concentrated overflow waters without substantial entrainment of North Atlantic waters or SSW bathing the site during H-events 1 – 3. Yet, the potential for overprinting of water mass Nd isotope signatures in this region (Lacan and Jeandel, 2004a; Roberts and Piotrowski, 2015), concerns about the fidelity of bulk sediment leachate Nd isotope records (Elmore et al., 2011; Wilson et al., 2013) and the range of water masses

influencing the intermediate-depth northeast North Atlantic (Lacan and Jeandel, 2005) are all sources of uncertainty demanding further careful assessment of the problem. Additional independent proxies of water mass provenance are therefore required to help reconstruct past vertical water mass structure from the Feni Drift.

To address these gaps in our knowledge, we report the results of a new multi-proxy reconstruction of bottom water chemistry and inferred water mass distribution from ODP Site 980. First, we present neodymium isotope reconstructions from three phases (fish debris, planktonic foraminifera and bulk sediment leachates), together with rare earth element distributions to better understand the controls on neodymium association with foraminifera at Site 980. Then we combine our Nd isotope reconstructions with new, high resolution records of three further proxies for water mass chemistry (B/Ca, $\delta^{13}\text{C}$ and $\delta^{18}\text{O}$ in benthic foraminifera) at our study site to shed new light on the response of the AMOC in the northeast North Atlantic to freshwater addition during four H-events of the last glacial period.

2. Background

2.1 Site Location and Oceanography

ODP Site 980 is situated on the Feni sediment drift, and features high sedimentation rates across the studied interval (mean 20 cm kyr⁻¹, see details of age model in supplementary material). Its position on the northern fringe of the main Atlantic belt of North American-sourced detrital carbonate deposition (Hemming, 2004) results in lithologically distinct and hence unambiguously identifiable Heinrich IRD layers. Site 980 is known for its

benchmark archives of millennial-scale climate variability during the Quaternary (e.g. McManus et al., 1999; Oppo et al., 2003; 2006, Fig. 2). Existing records from this site cover an unusually long interval for suborbitally resolved records, extending back approximately 500,000 years. Published data from Site 980 spanning the last glacial period are, however, of insufficient resolution to resolve changes in ocean chemistry across H-events clearly.

Today, Site 980 is bathed by a mixture of North East Atlantic Deep Water (NEADW) and Labrador Sea Water (LSW), with only a minimal influence of Wyville Thomson Ridge overflow waters (WTROW) from the Nordic Seas (Ellett and Martin, 1973; McGrath et al., 2012). During the last glacial period, Site 980 lay close to the interpreted depth of the boundary between northern- and southern-sourced waters (e.g. Boyle and Keigwin, 1987; Curry and Oppo, 2005; Oppo and Lehman, 1993), but is thought to have been bathed instead by Glacial North Atlantic Intermediate Water (GNAIW) during background glacial conditions (Yu et al., 2008). If AMOC shutdown occurred (as is classically suggested for last glacial H-events), model simulations suggest that Site 980 would have been bathed by Glacial Antarctic Bottom Water (GAABW) during these times (Flückiger et al., 2008; Singarayer and Valdes, 2010; Swingedouw et al., 2009).

2.2 Neodymium isotopes

Over the last few decades, neodymium isotopes have become an important tool for reconstructing the vertical structure of the water column and the provenance and circulation pathways of water masses. A major strength of the Nd isotope technique is

that, unlike many commonly used proxies for water mass chemistry (e.g. $\delta^{13}\text{C}$), neodymium isotopes are not influenced by biological processes. The estimated residence time of Nd in the ocean (200 – 1000 years (Arsouze et al., 2009; Tachikawa et al., 2003; Tachikawa et al., 1999)) is shorter than the modern oceanic mixing time of 1000 – 1600 years (e.g. Broecker and Peng, 1982; Garrison, 2011; Sarmiento and Gruber, 2004), giving rise to spatial variation in the isotopic signature of different water masses. Rocks exhibit a wide range of neodymium isotopic compositions, depending upon both their age and initial Sm/Nd ratios. These Nd isotope signatures are typically expressed in epsilon notation or ϵ_{Nd} (representing the $^{143}\text{Nd}/^{144}\text{Nd}$ deviation of a sample relative to a chondrite uniform reservoir in parts per 10,000) with values ranging from $\epsilon_{\text{Nd}} = -56$ for old granitic cratons to +12 for young mid-ocean ridge basalts (Jeandel et al., 2007; Lacan et al., 2012; Sarbas and Nohl, 2008, and references therein). Neodymium from this range of sources is transferred from the continents to the ocean via both riverine and aeolian inputs, resulting in different water masses acquiring distinct neodymium isotopic signatures (Goldstein et al., 1984; Grousset et al., 1992; Mearns, 1988; Tachikawa et al., 1999). Addition and exchange of neodymium at the sediment-bottom water interface along continental margins also modifies the neodymium isotopic signature of bottom waters through the process of boundary exchange (Lacan and Jeandel, 2004a; Rickli et al., 2014; Wilson et al., 2012).

Analysis of Fe-Mn oxyhydroxides within marine sediments extracted by a leaching procedure (e.g. Gutjahr et al., 2007; Rutberg et al., 2000) allows the production of relatively rapid and high resolution records of bottom water ϵ_{Nd} . This technique has now become widely used (e.g. Böhm et al., 2015; Jonkers et al., 2015; Wei et al., 2015;

Wilson et al., 2015). A wide range of other phases have also been proposed to record and preserve bottom water ϵ_{Nd} , including corals (e.g. Copard et al., 2010; van de Flierdt et al., 2006), ferromanganese nodules and crusts (e.g. O'Nions et al., 1978; Piepgras et al., 1979), fish debris (e.g. Lang et al., 2016; Martin and Haley, 2000; Staudigel et al., 1985) and foraminifera both with and without authigenic Fe-Mn oxide coatings (e.g. Elmore et al., 2011; Palmer and Elderfield, 1985).

The ϵ_{Nd} signatures recorded by different substrates do not always agree with one another (e.g. Elmore et al., 2011). For example, a pronounced difference between the glacial and Holocene ϵ_{Nd} values of uncleaned foraminifera is seen along a depth transect of Biogeochemical Ocean Flux Study (BOFS) cores on and to the south of the Rockall Plateau (Fig. 1), but this difference is muted or absent in co-registered bulk sediment leachate ϵ_{Nd} (Piotrowski et al., 2012). The leaching of bulk sediment can give a neodymium isotope signature influenced by reactive fine grained sediment components such as volcanic ash (which has a radiogenic signature) and detrital carbonate (which is unradiogenic) (Elmore et al., 2011; Roberts et al., 2010), and thus bulk sediment leachates may not accurately record bottom water chemistry at certain locations. The neodymium isotope signature extracted by bulk sediment leaching is also highly sensitive to the methodology used to separate the authigenic coating signal from the primary sediment (Wilson et al., 2013).

The mostly constant value of $\epsilon_{Nd} = -10$ recorded by bulk sediment leachates from Site 980 has been interpreted to demonstrate a continuous presence of WTROW in the Rockall Trough for most, if not all, of the last 40 kyrs due to the similarity of this value to the estimated signature of overflow waters (Crocket et al., 2011). In contrast, modern

oceanographic observations indicate only a minimal influence of WTROW at Site 980 today (Johnson et al., 2010; McGrath et al., 2012). Short-lived radiogenic Nd isotopic excursions identified in the Site 980 record with ages estimated as approximately concurrent to H-events 1 – 4 are inferred to record times of either increased influence of SSW during AMOC shutdowns or a more concentrated presence of overflow waters (Crocket et al., 2011). However, the limited resolution of the Site 980 bulk sediment leachate ϵ_{Nd} dataset and the absence of direct identification of H-layers in the site stratigraphy make these conclusions tentative (see also supplementary material). In addition, there are a number of other processes with the potential to alter bottom water ϵ_{Nd} (e.g. variable composition of NEADW or influence of LSW in the Rockall Trough, modification of bottom water isotopic signature by interaction with lithogenic material). The circulation history of the northeast Atlantic during the last glacial period therefore requires further investigation.

A decoupling between ϵ_{Nd} values and other proxies used as water mass tracers ($\delta^{13}C$, B/Ca (Yu et al., 2008)) suggests that the glacial-interglacial variability in foraminiferal ϵ_{Nd} on and to the south of the Rockall Plateau may not be a result of changing bottom water provenance (Roberts and Piotrowski, 2015). Instead, reactive IRD grains may modify water mass ϵ_{Nd} in this region as they sink through the water column, with large inputs of volcanic glass ($\epsilon_{Nd} = +4.3 \pm 0.1$) to the Rockall Plateau and its southern flank appearing to modify bottom water towards more radiogenic values during the Last Glacial Maximum (Roberts and Piotrowski, 2015). Unradiogenic labelling of the water column by Hudson Bay-derived detrital limestone grains ($\epsilon_{Nd} = -18.6 \pm 0.2$) may also have occurred during Heinrich events (Roberts and Piotrowski, 2015). These

observations raise questions over the temporal and spatial extent of water mass ϵ_{Nd} relabelling.

To better understand the meaning of bulk sediment ϵ_{Nd} data from Site 980 and to investigate whether issues of water column relabelling by IRD identified on the Rockall Plateau and its southern margin are applicable to a wider area of the northeast Atlantic, we therefore need higher resolution ϵ_{Nd} records from multiple phases at Site 980 supplemented by a record of concentrations and lithologies of IRD. Furthermore, independent proxies of bottom water chemistry are also required to improve our understanding of water mass structure of the northeast Atlantic during the last 41,000 years at Site 980, therefore we also present co-registered benthic $\delta^{13}C$, $\delta^{18}O$, B/Ca records.

3. Materials and Methods

3.1 Stratigraphy

We sampled Holes 980B (0.05 – 4.12 meters below seafloor (mbsf) at 8 cm resolution) and 980A (0.32 – 4.08 mbsf at 2 cm resolution). We sampled the same core sections as Crocket et al. (2011) to allow direct comparison with their data. Our Hole A samples are not part of the original primary shipboard splice (Shipboard Scientific Party, 1996), therefore, to assign composite depths (metres composite depth, mcd) to these samples, we correlated Hole A mbsf to the primary splice using shipboard-derived whole core volume-specific magnetic susceptibility data measured shipboard (see supplementary

information) (Shipboard Scientific Party, 1996). Our study interval corresponds to 0.06 – 8.12 mcd.

3.2 IRD and % *N. pachyderma* (s.)

Sediment samples were sieved at 150–500 μm , and then split until approximately 300 lithic grains remained, which were identified and counted using a binocular microscope, applying the categorizations of Hall et al. (2011). Pumice grains are assumed to have a volcanic ash origin, and so are not included in IRD counts. Reproducibility of IRD counts determined by repeat counts is $\pm 1\%$. IRD fluxes were estimated following Peck et al. (2007), with bulk density values corrected for a systematic error in the ODP Leg 162 shipboard gamma-ray attenuation porosity evaluator (GRAPE) measurements (Jansen et al., 2000). Samples prepared for IRD counts were then split again until approximately 300 foraminifera remained. Counts were performed of the number of specimens of *Neogloboquadrina pachyderma* (sinistral) in these splits and the value expressed as a percentage of the total number of planktonic foraminifera. Reproducibility of % *N. pachyderma* (s.) values determined by repeat counts is $\pm 3\%$.

3.3 Stable isotopes

To generate benthic stable oxygen and carbon isotope reconstructions for our target interval, specimens of *Cibicides wuellerstorfi* (typically 2 – 4) were picked from the $>212 \mu\text{m}$ size fraction (total carbonate mass 60 – 100 μg). Oxygen and carbon isotopic compositions of this carbonate were analysed using a Europa Geo 20-20 stable isotope ratio mass spectrometer at Southampton. All sample values are expressed in delta

notation, relative to the Vienna Peedee Belemnite standard (VPBD). External reproducibility is better than 0.053 ‰ for $\delta^{18}\text{O}$ and 0.027 ‰ for $\delta^{13}\text{C}$. Species-specific disequilibrium from seawater $\delta^{18}\text{O}$ values was removed by applying an adjustment of +0.64 ‰ (Shackleton and Opdyke, 1973). *C. wuellerstorfi* $\delta^{18}\text{O}$ values were adjusted for global sea level change ($\delta^{18}\text{O}_{\text{ivc}}$) to allow us to understand temporal changes in regional water mass chemistry, following the method of Meland et al. (2008) and using the sea level record shown in Grant et al. (2012) with a maximum glacial-interglacial sea level change of 110 m.

3.4 Neodymium isotope ratios, rare earth elements and trace elements

3.4.1 Sample preparation

To generate neodymium isotope and rare earth element profiles from foraminifera, a large number (600 – 1600) of planktic foraminifera of mixed species were picked in the >212 μm size fraction from each sample. These were broken open then sonicated in ELGA water and methanol to remove clays, before being dissolved in 1.75 M HCl. Ferromanganese coatings were not removed from the foraminifera, as these are rich in pore water-derived Nd and have been shown to record a bottom water signature (Elmore et al., 2011; Roberts et al., 2012).

Fish debris ϵ_{Nd} is considered to be a faithful recorder of the neodymium isotopic composition of bottom waters (e.g. Grandjean et al., 1987; Martin and Haley, 2000; Staudigel et al., 1985; Stille, 1992; Stille and Fischer, 1990). To provide an additional check on the fidelity of our new foraminiferal ϵ_{Nd} record, we therefore picked 1 – 15 pieces of fish debris from the >125 μm size fraction of a subset of samples ($n = 8$).

Adhering clays were removed by sonication in methanol and ELGA water. All samples were oxidatively cleaned based upon the methods of Boyle and Keigwin (1985), although a reductive cleaning step was not necessary (Martin and Haley, 2000). An aliquot of 10 μl was extracted from each of the dissolved foraminifera and fish debris samples for rare earth element (REE) and other trace element analysis, with the remainder of the sample used for neodymium isotope analysis.

3.4.2 Rare and trace elements

The mechanism by which Nd becomes associated with foraminifera strongly influences whether the isotopic signature preserved is representative of the bottom water signature (Roberts et al., 2012; Tachikawa et al., 2014). The extent of remobilization of Nd in sediment pore waters is of particular interest, and can be investigated using REE concentrations and distributions (Roberts et al., 2012). Subtle differences in the behaviour of the various REEs result from a decrease in atomic radius as mass increases, leading to differences in their speciation in seawater (Elderfield and Greaves, 1982; Goldberg et al., 1963). The behaviour of cerium is also distinct from the other elements because it can be oxidized from a soluble (3+) to an insoluble (4+) state (de Baar et al., 1985; Elderfield et al., 1988). This distinction can be expressed by the cerium anomaly (Ce/Ce^*), which is the difference in the shale-normalised abundance of cerium compared to the expected value calculated from the nearby light rare earth (LREE) elements ($\text{Ce}/\text{Ce}^* = 3\text{Ce}_n / (2\text{La}_n + \text{Nd}_n)$, where $_n$ indicates concentrations relative to the Post-Archean Australian Shale, PAAS (McLennan, 1989; Taylor and McLennan, 1985)). Negative cerium anomalies (values <1) indicate a depletion of cerium relative to the other REEs

(de Baar et al., 1988).

Rare earth element samples were diluted with 3% HNO₃ spiked with In, Re and Be. Calcium and strontium concentrations were measured with a Quadrupole ICP-MS: Thermo X-Series 2 at Southampton. The remaining sample solutions were analysed for REE and trace element concentrations by High Resolution ICP-MS: Thermo ELEMENT 2XR at Southampton. All samples were corrected for matrix effects and instrument drift using the In, Re and Be standard incorporated into each sample. A blank correction was then applied and rare earth element standards used to correct samples for oxide formation. External reproducibility is estimated as 4–5 %, with internal reproducibility much less than this for the majority of samples. Rare earth element concentrations of the samples (REE_{sample}) were expressed relative to the REE signature of the PAAS (REE_{PAAS}) (McLennan, 1989; Taylor and McLennan, 1985).

3.4.3 Neodymium isotope ratios

Neodymium was purified from the dissolved samples for isotope analysis using standard procedure column chemistry, based upon the methods of Cohen et al. (1988). Cation columns were used to strip iron and titanium from the samples. The remaining material was then run through LN SpecTM columns to purify and concentrate neodymium (Pin and Zalduegui, 1997). Samples were analysed by Multi-collector ICP-MS: Thermo NEPTUNE at Southampton. Instrumental mass bias ratios were corrected using the procedure of Vance and Thirlwall (2002), adjusting to a ¹⁴⁶Nd/¹⁴⁴Nd of 0.7219 and using cerium-doped standards to correct for interference of ¹⁴²Ce on ¹⁴²Nd. All values were normalised to the JNdi-1 Standard (¹⁴³Nd/¹⁴⁴Nd = 0.512115±7) (Tanaka et al., 2000), and

isotopic signatures are expressed in epsilon notation, using a chondritic uniform reservoir value of 0.512638 (Jacobsen and Wasserburg, 1980). Replicate measurements of the JNdi-1 standard across the three analytical sessions gave an external reproducibility 2 s.d. = 0.2 ϵ_{Nd} units for replicate analyses of Nd standard solutions (n = 25). Error bars plotted show either this external reproducibility or the sample internal reproducibility, whichever is larger. We compared our Nd data to co-measured concentrations of lithophilic elements (e.g. Al, Ti, Zr, Pb) and volcanic grains, and found no evidence to suggest a strong influence of volcanic ash, clay contamination or other terrestrial material on foraminiferal ϵ_{Nd} values at Site 980 (see supplementary information).

3.5 Boron/calcium ratios

Between 8 and 12 *C. wuellerstorfi* tests (212 – 500 μm) were cleaned for trace metal analysis following Barker et al. (2003). Foraminiferal tests were cracked and ultrasonicated in Milli-Q 18.2 M Ω -cm water to remove clay materials. Samples were then oxidatively cleaned in a 1% hydrogen peroxide solution before a weak acid leach was applied to remove adsorbed cations. Finally, samples were dissolved in ~ 0.075M nitric acid. The above steps were all undertaken in a specialised boron free clean laboratory at the University of Southampton. Element ratios were measured using a ThermoFisher Scientific Element 2XR-ICPMS at Southampton, using the protocol described by Rae et al. (2011) employing matrix-matched in house standards and a variety of consistency standards to ensure reproducibility. Samples were screened for clay contamination using Al/Ca and other contaminant ratios (e.g. Ba/Ca, Fe/Ca), with samples Al/Ca > 100 $\mu\text{mol/mol}$ excluded from this study (n = 2). No anomalous values of other elements were

identified. Near complete clay removal is assumed for the remaining samples. Long-term reproducibility for B/Ca during this study was within 4 % at 2 s.d. ($\sim 8 \mu\text{mol/mol}$). Carbonate ion concentrations were calculated using a sensitivity of $\Delta[\text{CO}_3^{2-}]$ on B/Ca of 1.14 ± 0.048 for *C. wuellerstorfi* (Yu and Elderfield, 2007), and a $[\text{CO}_3^{2-}]_{\text{sat}}$ calculated from modern local pressure, temperature and salinity.

3.6 Age model generation

A new age model was developed for Site 980 by combining previously published radiocarbon ages (Benway et al., 2010; Oppo et al., 2003) with a new record of the abundance of planktonic foraminifera *N. pachyderma* (s.) correlated to Greenland proxy records (Fig. 2 and supplementary information). An average sedimentation rate of ~ 0.2 mm/yr means that samples with 2 cm spacing give an age resolution of approximately 100 years.

Radiocarbon ages were updated using the Marine13 calibration curve (Reimer et al., 2013) in conjunction with Calib 7.1 software (Stuiver and Reimer, 1993; Stuiver et al., 2005). A constant reservoir age of 400 ± 100 years was assumed, with the exception of the Younger Dryas (800 ± 300 years) and H1 (1600 ± 1000) (e.g. Bard, 1988; Bard et al., 1994; Bondevik et al., 2006; Stanford et al., 2011; Stern and Lisiecki, 2013; Waelbroeck et al., 2001). Additional age constraints were provided by correlating the Site 980 % *N. pachyderma* (s.) record (a proxy for upper ocean temperature when sea surface temperatures are between 4°C and 10°C (Darling et al., 2006)) to North Greenland Ice Core Project (NGRIP) $\delta^{18}\text{O}_{\text{ice}}$ (a proxy for atmospheric temperatures) (North Greenland Ice Core Project Members et al., 2004) on the GICC05 age model (Andersen et al., 2006;

Rasmussen et al., 2006; Svensson et al., 2008; Vinther et al., 2006). Visual correlation was carried out using the Analyseries software (Paillard et al., 1996), and is based on the assumption that temperature changes in the upper North Atlantic Ocean were synchronous with Greenland air temperatures. Distinctive peaks in detrital carbonate fluxes were used to confirm the position of H4, H2 and H1.

4. Results and Discussion

4.1 Assessing neodymium isotopes as a water mass tracer at ODP Site 980

4.1.1 Exploring inter-substrate differences in neodymium isotope signatures

New records of REE distributions and Nd isotope signatures of mixed planktonic foraminifera and fish debris from Site 980 are shown together with IRD concentrations in Fig. 3. Throughout our study interval, there is close agreement between new data from fish debris and planktonic foraminifera ϵ_{Nd} data. Glacial ϵ_{Nd} values recorded by fish and foraminifera (-9 to -10) are more radiogenic than Holocene values (~ -11.5), with suborbital unradiogenic excursions from baseline values during H4 (~ 38 ka) and the early Holocene ($\sim 5 - 8$ ka), and a strong radiogenic excursion across H2 ($\sim 23 - 26$ ka) (Fig. 3a). Previously published sediment leachate ϵ_{Nd} data from Site 980 (Crocket et al., 2011) generally show a systematic offset towards more radiogenic values than our new foraminifera and fish debris values by $1 - 2 \epsilon_{Nd}$ units over the last ~ 11.5 ka (Fig. 3a). This systematic offset is not present in the samples of peak glacial age, where agreement

between the two substrates is often much closer, although there are some sporadic disagreements between the two records.

Modern oceanographic observations show that the mid-depth western Rockall Trough is predominantly bathed by NEADW ($\epsilon_{Nd} = -12.8 \pm 0.2$) and LSW (-13.9 ± 0.4), with a small influence of overflow waters from the Nordic Seas (-8.2 ± 0.6) (Ellett and Martin, 1973; Johnson et al., 2010; Lacan and Jeandel, 2005; McGrath et al., 2012; Olsen and Ninnemann, 2010). This suggests that the youngest foraminiferal ϵ_{Nd} values at Site 980 (-11.7 ± 0.3) capture bottom water chemistry more accurately than bulk sediment leachate ϵ_{Nd} (-10.2 ± 0.3). A stronger overflow signature than indicated by modern observations (Johnson et al., 2010) or local modification of bottom waters towards more radiogenic values is required if the youngest leachate ϵ_{Nd} signatures at our study site accurately represent recent bottom water chemistry. Alternative explanations include analytical issues offsetting the bulk sediment leachates to more radiogenic values than the fish debris and foraminifera, and the influence of an additional radiogenic phase shifting bulk sediment leachates towards more radiogenic values in the Holocene.

Bulk sediment leachates can provide a relatively rapid way to reconstruct seawater chemistry, but a number of studies have highlighted the sensitivity of the technique to the precise method used. Wilson et al. (2013) and Blaser et al. (2016) have recently shown that carbonates play an important role as a buffer when extracting the ferromanganese coatings from sediments, preventing the acid-induced mobilization of Fe oxides and volcanogenic material (which has the potential to shift the measured ϵ_{Nd} towards more radiogenic values). Crocket et al. (2011) followed the earlier procedure of Gutjahr et al. (2007) which included a prior decarbonation step. Leaching time, sample

size and pH have also been shown to influence the bulk sediment leachate ϵ_{Nd} signature (Blaser et al., 2016; Wilson et al., 2013)

Radiogenic offsets of bulk sediment leachate ϵ_{Nd} values from foraminiferal Nd signatures have also been documented in core top samples at other sites in the North Atlantic and attributed to the influence of volcanic ash that is easily leached during the extraction process (Elmore et al., 2011). There is no evidence, however, for increased or sustained volcanic activity throughout the Holocene that would increase the accumulation rate of ash in the sediment at Site 980 (see supplementary information). Instead, North Atlantic ash deposition is much more frequent during the last deglaciation (e.g. Abbott and Davies, 2012; Davies et al., 2012; Lowe et al., 2008), when very good agreement exists between foraminiferal and bulk sediment leachate ϵ_{Nd} at Site 980. Airborne volcanic ash therefore cannot easily be invoked to explain the observed offset between substrates during the Holocene.

Variable transport of silt-sized titanomagnetite grains from the GSR by bottom currents has been documented at a number of sediment drift sites that lie in the path of overflow waters. Higher accumulation of titanomagnetite is documented associated with higher current velocities under interstadial conditions compared to stadials, with grains likely originating from the young basaltic (and radiogenic) rocks of the Nordic Basaltic Province (Ballini et al., 2006; Kissel, 2005; Kissel et al., 1999). Bottom currents were generally much stronger in the Holocene than the glacial in the North Atlantic (Innocent et al., 1997; Manighetti and McCave, 1995; McCave et al., 1995a; McIntyre and Howe, 2009; McManus et al., 2004; Thornalley et al., 2013), therefore, increased accumulation of leachable fine material at the Feni Drift during the Holocene represents a possible

alternative explanation for the more radiogenic signature recorded by Site 980 sediment leachates. There is a possibility that certain other drift deposits in the region may be susceptible to a similar process because the spatial distribution of sites showing unreasonably radiogenic core top sediment leachate ϵ_{Nd} values (as identified by Elmore et al. (2011)) agrees well with the major pathways of modern Nordic Overflow waters (e.g. Hansen and Østerhus, 2000), and bulk sediment leachate ϵ_{Nd} records showing the largest radiogenic offset compared to other substrates during the Holocene have been reported at some other sites in the North Atlantic (Piotrowski et al., 2012; Roberts et al., 2010).

We conclude that the influence of bottom current transported, silt-sized radiogenic particles on sediment leachate ϵ_{Nd} is the most likely explanation for the offset between the Nd isotope substrates during the Holocene at our study site, with the leachate method also contributing to the variable offsets throughout the record. This implies that published bulk sediment leachate values are not an accurate record of bottom water chemistry at Site 980, at least in the uppermost sedimentary column (above 2.9 mcd). As a consequence, we only consider the Nd isotopic signatures of foraminifera and fish debris as potential tracers of water mass provenance at Site 980.

4.1.2 Controls on downcore rare earth element distributions

The downcore REE signatures of planktonic foraminifera at Site 980 (shown in Fig. 3b–f) are characterized by upper (zone I) and lower (zone II) intervals with a distinct transition at 2.9 mcd (11.5 ka). Nd/Ca values (Fig. 3b) are consistently relatively low throughout zone I (~700 – 800 nmol/mol), with higher and more variable values in zone II (900 – 3000 nmol/mol). Nd/Mn values are also more variable in zone II, with the highest values

typically associated with (or close to) H-events. Below the transition at 2.9 mcd, there is less enrichment of heavy REEs over light REEs (Fig. 3e) and cerium anomaly values are closer to 1 (Fig. 3d). A systematic offset between the sediment leachate ϵ_{Nd} values and the other substrates is also recorded in zone I but is not clearly present in zone II (Fig. 3a). This observation raises the possibility of a link between the processes controlling REE distributions across 2.9 mcd and inter-substrate offsets in ϵ_{Nd} values. We explore three potential explanations for the distinct difference in behavior of REEs in the upper (zone I) and lower (zone II) sections of the studied interval. These are (i) exchange between detrital and authigenic phases, (ii) an active redox front in the sediment and (iii) preserved differences between glacial and interglacial bottom water chemistry.

The REE signature of bulk sediment can co-vary with lithology (e.g. Sholkovitz, 1988). The detrital fraction, however, is typically unreactive, as evidenced by its extraction procedure (Bayon et al., 2002; Jones et al., 1994), and REE concentrations are much lower than in the Fe-Mn oxyhydroxide fraction (Gutjahr et al., 2007). The ϵ_{Nd} values of bulk sediment at Site 980 (Crocket et al., 2011) are consistently offset towards less radiogenic values than any of the substrates discussed here (Fig. 3a). There is also no clear relationship between the relative proportions of radiogenic and unradiogenic IRD and the co-registered foraminiferal ϵ_{Nd} (see supplementary information). These observations suggest that significant exchange between the detrital and authigenic phases is not the main control on foraminiferal REE distributions.

Many of the phases which have been shown to host REEs associated with foraminifera (Fe-Mn (hydr)oxides, organic matter and Mn carbonates) are sensitive to redox conditions (Tachikawa et al., 2014). Therefore, the presence of an active redox

front at 2.9 m depth could result in a remobilization and redistribution of foraminiferal REEs. The similarity of shift in REE distribution recorded by both foraminifera and fish debris, however, argues against this explanation at Site 980. The REE signal of fish debris is acquired at shallow depths in the sediment and is relatively resistant to diagenesis, with substitution of rare earth elements into the crystal lattice occurring only under more extreme conditions and resulting in a distinctive bell-shaped REE profile (Martin and Scher, 2004; Reynard et al., 1999; Staudigel et al., 1985). This profile is not seen in any of the samples presented here (Fig. 4). In addition, strong negative Ce/Ce* values are preserved in Miocene fish teeth at nearby Site 982 (Martin et al., 2010), similar to that preserved by Holocene (but not glacial) samples at Site 980, suggesting that REE distributions are not reset below the top few metres of sediment. Therefore, it is unlikely that diagenetic redistribution across an active redox front explains the shift in REE distribution in either uncleaned foraminifera or fish debris, supporting our use of fish debris and foraminiferal REE chemistry at Site 980 to reconstruct past oceanographic conditions.

The cerium anomaly (Ce/Ce*) is often used to track oxidation because cerium is readily converted from the insoluble Ce (IV) to the soluble Ce (III) phase when water column oxygenation decreases (Elderfield et al., 1988). It should, however, be noted that Ce/Ce* preserved by sediment components is not an infallible recorder of local bottom water oxidation, with questions raised regarding the incorporation of REEs into various marine substrates (e.g. German and Elderfield, 1990; Holser, 1997; MacLeod and Irving, 1996). In addition, lower Ce/Ce* ratios are recorded in the modern Pacific and Indian Oceans compared to the North Atlantic Ocean; a result which is attributed to a

progressive removal of Ce as the age of a bottom water mass increases (German and Elderfield, 1990). The higher Ce/Ce* values at Site 980 during the glacial could therefore indicate a more vigorous overturning circulation than during the Holocene, with several studies supporting vigorous renewal of intermediate waters in the North Atlantic under glacial conditions (e.g. Gherardi et al., 2009; McCave et al., 1995a). An alternative explanation is that the higher Ce/Ce* values in zone II (close to 1; Fig. 3d) in our record indicate that glacial bottom waters at Site 980 had a relatively low oxygen content compared with conditions in the Holocene. A similar increase in both Ce/Ce* and Nd/Ca of uncleaned planktonic foraminifera during the transition into the Holocene has been recorded at Bermuda Rise (Roberts et al., 2012). Glacial-interglacial differences in the degree of oxygenation of shallowly buried sediments have been documented in a number of studies around the world (Jaccard and Galbraith, 2012), with decreased oxygenation of glacial bottom waters reported in the intermediate depth northeast Atlantic (Baas et al., 1998; Schönfeld et al., 2003). The broad coincidence of the boundary between zone I and II with the climatic transition into the Holocene therefore raises the possibility that the differences in REE behaviour at Site 980 are the product of differences in the degree of pore water oxidation between glacial and interglacial conditions.

4.1.3 Assessing the influence of water mass labelling by IRD at Site 980

Foraminiferal ϵ_{Nd} values during the late Holocene (-11.7 ± 0.3) at Site 980 are consistent with the representative signatures of the water masses bathing this site today but determining whether older ϵ_{Nd} signatures are also representative of regional water mass chemistry requires further evaluation. The radiogenic signal (-7.9 to -4.2) in

foraminiferal ϵ_{Nd} of the nearby BOFS cores (locations shown in Fig. 1) during the Last Glacial Maximum has been interpreted to reflect labelling of the bottom waters bathing these sites by IRD raining through the water column (Roberts and Piotrowski, 2015). Therefore, before we can use foraminifera-based ϵ_{Nd} data from Site 980 to determine past variations in water mass sourcing, first we must explore the possibility that exchange with lithogenic material has influenced glacial ϵ_{Nd} values in our datasets.

Three lines of evidence suggest that there was a smaller influence of local modification of water mass chemistry by IRD at ODP Site 980 than the BOFS sites. First, the radiogenic ϵ_{Nd} values (≥ -8) reported by Roberts and Piotrowski (2015) during MIS 2 are not recorded at Site 980 (Fig. 5a). Second, we observe ϵ_{Nd} excursions of opposing signs during H2 and H4, despite lithologically similar IRD assemblages (Fig. 3a and supplementary information). Third, our new IRD records demonstrate that IRD inputs during the last glacial period at Site 980 (typically 0 – 650 grains/g, peaking at 1450 grains/g during H2) are lower than those recorded at the BOFS sites (400 – 4700 grains/g, (Roberts and Piotrowski, 2015)) (Fig. 5c and d). The same result is also true of the concentrations of volcanic grains, highlighting that the Feni Drift was likely subject to a different IRD depositional regime than the one influencing the BOFS sites during the last glacial period. Although we cannot discount the influence at Site 980 of water masses modified by IRD upstream of our site, and no direct correlation was found between volcanic IRD concentration and ϵ_{Nd} values by Roberts and Piotrowski (2015), we suggest that the absence of large volumes of reactive material sinking through the water column at Site 980 during the last glacial period reduced the potential for local modification of water mass chemistry. We therefore suggest that IRD water mass relabelling is not the

dominant control on the down core variability in our ϵ_{Nd} data. Hence, modification of the water column ϵ_{Nd} by IRD (Roberts and Piotrowski, 2015) may not be significantly problematic in all regions of IRD deposition.

4.2 Water mass changes

Having established that fish debris and uncleaned planktic foraminifera provide a reliable record of bottom water Nd isotope composition at ODP Site 980, next we combine these ϵ_{Nd} data with three other proxies for water mass chemistry (B/Ca, $\delta^{13}\text{C}$ and $\delta^{18}\text{O}$) to reconstruct oceanographic variability in the mid-depth northeast North Atlantic over the past 41,000 years.

4.2.1 Glacial-interglacial variability

In Fig. 6, we present Site 980 fish debris and foraminiferal ϵ_{Nd} alongside benthic $\delta^{13}\text{C}$ and B/Ca ratios for the past 41 kyrs. A distinct difference in the properties of the water mass bathing Site 980 can be seen between the glacial and Holocene, with glacial waters having a more radiogenic ϵ_{Nd} signature (Fig. 6b), slightly lower carbon isotope values (Fig. 6c) and higher $[\text{CO}_3^{2-}]$ (indicated by higher benthic foraminiferal B/Ca ratios, Fig. 6a). These observations strongly suggest that the interpretation of Crocket et al. (2011) invoking the persistent dominance of WTROW throughout the last 40 kyr at this site cannot be correct without a significant shift in the properties of WTROW.

Marked similarities exist between the long-term evolution of ϵ_{Nd} at Site 980 and deep water sites at the Bermuda Rise (Böhm et al., 2015; Gutjahr and Lippold, 2011; Roberts et al., 2010) and South Atlantic Cape Basin (Piotrowski et al., 2012; Piotrowski

et al., 2005; Rutberg et al., 2000) (Fig. 7). The Bermuda Rise and Cape Basin records are primarily controlled by mixing between unradiogenic northern- and radiogenic southern-sourced waters. An increased contribution of radiogenic southern-sourced waters mixing with northern-sourced waters in the glacial northeast North Atlantic cannot be ruled out on the basis of Nd isotopes alone, but B/Ca-based reconstructions of carbonate ion concentrations argue against this interpretation. Both modern and glacial SSW typically have low $[\text{CO}_3^{2-}]$ (75 – 95 $\mu\text{mol/mol}$), whereas modern North Atlantic Deep Water and Nordic Sea overflows are much richer in $[\text{CO}_3^{2-}]$ (>100 $\mu\text{mol/mol}$) (Key et al., 2004; Yu et al., 2014; Yu et al., 2008). Reconstructed glacial carbonate ion concentrations (~130 – 150 $\mu\text{mol/mol}$) at Site 980 are higher than those in the Holocene (~115 – 135 $\mu\text{mol/mol}$) (Fig. 6), the opposite direction of change as would be expected if an increased glacial presence of southern-sourced waters is the dominant driver of the difference in bottom water chemistry observed at Site 980 between the Holocene and last glacial period.

A reduction in the influence of unradiogenic LSW under glacial conditions (Cottet-Puinel et al., 2004; Hillaire-Marcel et al., 2001) could contribute to the more radiogenic glacial ϵ_{Nd} signature at Site 980, however, as modern LSW has high $[\text{CO}_3^{2-}]$ (Key et al., 2004; Yu et al., 2008), a decrease in glacial LSW influence alone cannot explain the observed bottom water chemistry changes at Site 980 if it is assumed that glacial LSW had similar properties to modern. A decreased export of Mediterranean outflow water (MOW) has been documented under glacial conditions (Zahn et al., 1997), but as modern MOW is moderately radiogenic (-9.4 ± 0.5 (Spivack and Wasserburg, 1988)), a reduction in MOW cannot explain the glacial shift towards more radiogenic bottom waters at Site 980. Alternatively, Rogerson et al. (2005) suggest that the core of

MOW deepened which could increase its influence at Site 980, and as MOW has a high modern $[\text{CO}_3^{2-}]$, potentially contribute to the observed shift in glacial-interglacial bottom water chemistry. An increased influence of relatively radiogenic and high $[\text{CO}_3^{2-}]$ Nordic Sea overflow waters at Site 980 during the last glacial period as suggested by Yu et al. (2008) is an alternative candidate to explain the more radiogenic and $[\text{CO}_3^{2-}]$ -rich glacial bottom water signature at Site 980. It should be noted that an increased influence of overflow waters on bottom water chemistry at Site 980 does not require an increase in overflow current vigour, particularly in light of the decreased contribution of LSW (Cottet-Puinel et al., 2004; Hillaire-Marcel et al., 2001) to the main Atlantic basin during the last glacial period.

4.2.2 Heinrich events

Our multi-proxy reconstruction of bottom water properties at Site 980 shows prominent excursions associated with increased concentrations of IRD during each of H-events 4 – 1 (Fig. 6). Large shifts in the ϵ_{Nd} of bottom waters are documented for both H4 ($\epsilon_{\text{Nd}} = -13.6$) and H2 (-7.1), but these excursions are of opposing signs. A small ($\sim 20 \mu\text{mol/kg}$) reduction in bottom water $[\text{CO}_3^{2-}]$ is recorded during H2 and just prior to H3, but there is no significant change during H4, and at no point in the record do the values get close to SSW values of $75 - 95 \mu\text{mol/kg}$ (Key et al., 2004; Yu et al., 2014; Yu et al., 2008). Excursions towards low benthic $\delta^{13}\text{C}$ are recorded during each of the H-events, although typically lagging slightly behind the main IRD peak.

Arguably, the most notable feature is the unique expression of each event in our proxy records of bottom water chemistry, with differences in the sign of change, as well

as the magnitude of excursions. This simple observation shows that circulation changes in the mid-depth glacial northeast Atlantic are much more complex than simple two component northern- and southern-sourced endmember mixing model. Instead, either three or more water masses must have influenced Site 980 during the last glacial period, or alternatively, shifts in surface ocean properties (particularly in deep water formation regions) or circulation vigour significantly modified the properties of water masses.

The surface of the North Atlantic Ocean is thought to have been a highly dynamic environment during the last glacial period, with temporally variable freshwater input from both icebergs and continental sources (Heinrich, 1988; Hemming, 2004; Lekens et al., 2006; Stanford et al., 2011). Fluctuations in sea surface temperature, salinity, sea ice cover and productivity have all been documented in the high northern latitudes (e.g. Dokken et al., 2013; Maslin et al., 1995; van Kreveld, 1996). An increase in sea ice cover has the potential to reduce air-sea exchange in the deep water formation regions, with CO₂ invasion and evasion acting upon both the $\delta^{13}\text{C}$ and carbonate ion concentration of a water mass in a specific ratio (Fig. 8) (Yu et al., 2008). The variability in our data between H-events and non-Heinrich glacial intervals does not follow this trend, therefore we infer that variable sea-ice cover in deep water formation regions is not a major contributor to the variability in bottom water chemistry recorded at Site 980 during H-events. Instead, there is a closer fit to the “biology” slope, which represents the influence of biological regeneration on seawater chemistry and incorporates the effects of organic tissue degradation and CaCO₃ remineralisation (Yu et al., 2008). The influence of a water mass with increased organic matter remineralisation may therefore explain part of the H-event signals in our proxy records. This signature could reach the site either by increased

surface productivity or increased age of the bottom waters reflecting a longer time interval since the water mass was exposed to the atmosphere, either as a result of a rearrangement of circulation patterns, a shift in water mass boundaries or a decrease in circulation vigour. Additional independent proxy records for current vigour such as such as sortable silt (McCave et al., 1995b) or $^{231}\text{Pa}/^{230}\text{Th}$ (Yu et al., 1996) could therefore prove valuable in better understanding the origin of the observed excursions of bottom water chemistry in the northeast North Atlantic during H-events.

4.2.2.1 Heinrich event 4

Heinrich event 4 is distinct from the other H-events in our record because it is characterized by an excursion towards unradiogenic ϵ_{Nd} values and a notable decrease in benthic foraminiferal $\delta^{18}\text{O}$ (Figs. 6d and 9). Similar $\delta^{18}\text{O}$ excursions have been linked to episodes of brine formation in the Nordic Seas (Dokken and Jansen, 1999; Meland et al., 2008; Vidal et al., 1998), although the origin of the low $\delta^{18}\text{O}$ signature is debated (e.g. Bagniewski et al., 2015; Bauch and Bauch, 2001; Rasmussen and Thomsen, 2009; Stanford et al., 2011). Regardless, a Nordic Sea origin for the waters bathing Site 980 during H4 can likely be discounted because modern Nordic Seas Overflows have radiogenic signatures of $\epsilon_{\text{Nd}} = -8.2 \pm 0.6$ (Lacan and Jeandel, 2004b) while our data record a shift of $\sim 2 \epsilon_{\text{Nd}}$ units towards more unradiogenic values. A very large shift in the neodymium isotope composition of the Nordic Seas (for example, due to overprinting by unradiogenic IRD from Greenland) would be required for the shift in bottom water chemistry recorded at Site 980 to be attributed to increased presence of Nordic Seas Overflows at the site. The main source of unradiogenic waters in the North Atlantic today

is the Labrador Sea. LSW generation is thought to have been weaker during the last glacial period, although with some evidence of sinking of brine-rich waters during Heinrich events (Cottet-Puinel et al., 2004; Hillaire-Marcel and de Vernal, 2008; Hillaire-Marcel et al., 2001; Nuttin et al., 2015; Weber et al., 2001).

Alternatively, an increase in deep water formation south of the GSR could explain the ϵ_{Nd} signal at Site 980 during H4 (Duplessy et al., 1980; Labeyrie et al., 1992). Surface waters today in the northeast North Atlantic have ϵ_{Nd} values of -13 to -14.8 (Lacan and Jeandel, 2004c), although southward migration of the polar front during H-events (e.g. Eynaud et al., 2009) may have resulted in more radiogenic surface water signatures. Reconstructions of surface water properties in the open ocean suggest that they may have been insufficiently dense to sink (Maslin et al., 1995). Alternatively, brine formation, could have occurred on the European and/or Icelandic margins, Rockall Plateau or GSR (Meland et al., 2008; Thornalley et al., 2010), with a possible additional input of waters with low $\delta^{18}O$ and $\delta^{13}C$ signatures from the European continent (e.g. Eynaud et al., 2007; Toucanne et al., 2009).

4.2.2.2 Heinrich event 2

Heinrich event 2 shows a very different signal to H4 in our multi-proxy records. Unlike H4, there is no $\delta^{18}O$ excursion (Fig. 6d), and ϵ_{Nd} values shift ~ 2 units towards more radiogenic values (> -8 ; Fig. 6b). A combination of radiogenic ϵ_{Nd} and low $\delta^{13}C$ with no concurrent excursion in $\delta^{18}O$ in the Atlantic basin is commonly associated with SSW in the Atlantic (e.g. Jonkers et al., 2015; Piotrowski et al., 2008; Rutberg et al., 2000; Thornalley et al., 2010). We also see a small decrease in carbonate ion concentrations

(~20 $\mu\text{mol/kg}$), which supports an increase in the contribution of southern-sourced waters to the northeast North Atlantic. Our reconstructed $[\text{CO}_3^{2-}]$ of > 120 $\mu\text{mol/kg}$ at Site 980 during H2 is, however, well above modern Antarctic bottom and intermediate waters (~ 85 $\mu\text{mol/kg}$) (Key et al., 2004; Yu et al., 2008), and even more discrepant with values of ~ 80 $\mu\text{mol/kg}$ reported for deep SSW during the Last Glacial Maximum (Yu et al., 2014), so any southern-sourced water would need to be highly diluted by mixing with northern-sourced endmembers. An alternative source of radiogenic waters with high $[\text{CO}_3^{2-}]$ is the Nordic Seas (Lacan and Jeandel, 2004b; Lacan et al., 2012), a possibility consistent with proposed strengthening of GSR overflows into the North Atlantic during H-events (Crocket et al., 2011; Meland et al., 2008; Thornalley et al., 2010).

A clear temporal lag (~ 2 kyr, represented by 30 cm of core) exists between the onset of excursions in ϵ_{Nd} and $\delta^{13}\text{C}$ during H2 (Fig. 10). The initial shift in ϵ_{Nd} values appears to lead the IRD flux increase slightly (as also observed by Gutjahr and Lippold (2011)), suggesting that major freshwater release linked to IRD deposition across the North Atlantic is not required to initiate the circulation changes associated with H-events, although we cannot rule out the influence of earlier, smaller-scale freshwater releases in other locations. A similar result was obtained by Barker et al. (2015) who find that meltwaters from icebergs do not trigger Northern hemisphere stadial events. Bottom water $[\text{CO}_3^{2-}]$ values only start to decrease when stadial conditions are well established. The delayed excursion towards low $\delta^{13}\text{C}$ values could be a result of a local or regional pulse in the flux of organic matter to the seafloor (Mackensen et al., 1993), or the flushing of previously poorly ventilated waters once ice-rafting has ceased and circulation vigour is increasing. Alternatively, the observed lag may indicate the presence of multiple

phases of AMOC reorganization (Wilson et al., 2014), involving the existence of short-term circulation modes, rather than a simple switch between two distinct AMOC states ('glacial' and 'off') (Rahmstorf, 2002).

4.2.2.3 Exploration of the differences between H-events

Comparison between multiple H-events allows greater insight into the processes governing AMOC response to fresh water additions. The results of two recent studies (Böhm et al., 2015; Lynch-Stieglitz et al., 2014) suggest that an important role in determining the magnitude of oceanographic response to freshwater input is played by the stage in the glacial cycle at which freshwater was released. One of these studies, based on reconstruction of flow through the Florida Straits, suggests that AMOC was least sensitive to freshwater forcing during full last glacial conditions when stratification of the Atlantic Ocean was at its greatest (Lynch-Stieglitz et al., 2014). The other, a study of water chemistry in the deep North Atlantic on Bermuda Rise, suggests that during the last glacial cycle, the greatest AMOC weakening only occurs when a threshold in continental ice sheet size is crossed, with ice volumes close to their maximum (Böhm et al., 2015). While the magnitude of AMOC perturbation cannot be simply gauged by the amplitude of the excursion in our proxy records, the variability across our data sets strongly suggests a discernible reorganization in ocean structure associated with both H2 (which occurs at close to peak glacial conditions) and H4 (when ice sheets were much smaller (e.g. Siddall et al., 2003)). Our results therefore offer a different perspective, suggesting that the stage of the glacial cycle occupied by H-events may not be the

principle factor governing the response of the mid-depth North Atlantic to freshwater release.

The unique chemical signature of intermediate waters during each of the H-events examined (H4 to H1) at Site 980 therefore requires an alternative explanation to changes in global ice volume. Differences in the location, duration and magnitude of melt water inputs have been shown to exert a clear influence over the response of AMOC in modelling experiments (Bigg et al., 2011; Otto-Bliesner and Brady, 2010; Smith and Gregory, 2009). Differences in the IRD assemblages have been documented between H-events (e.g. Grousset et al., 1993; Hall et al., 2011; Peck et al., 2007; Snoeckx et al., 1999), most notably a decreased flux of Hudson Bay-sourced detrital carbonates reaching the North Atlantic during H3 and H6 (e.g. Bond et al., 1992; Hemming, 2004; Hodell and Curtis, 2008), suggesting differences in the relative fresh water contributions from the circum-Atlantic ice sheets. Each H-event is therefore likely associated with different volumes, rates and/or delivery routes of freshwater to the North Atlantic Ocean. These differences are likely to have resulted in shifts in the relative strength of surface water subduction in a number of different potential deep water formation areas. This interpretation of events also offers a potential explanation as to why different events have a different prominence in different locations, and therefore why records from different study regions point to different relationships between global ice volume and AMOC stability (Böhm et al., 2015; Lynch-Stieglitz et al., 2014). AMOC strength has also been shown to exert a strong control over continental hydroclimate (e.g. Burckel et al., 2015; Mulitza et al., 2008), therefore, variations in meltwater inputs between H-events and the resulting AMOC perturbations may have important implications for terrestrial climate.

The unique response of intermediate water to fresh water input during each H-event examined (4 to 1) also raises the possibility of variations in the properties of GNAIW during H-events; a result that may have implications for downstream reconstructions of the strength of exported water from the high northern latitudes at these times. Glacial bottom water chemistry at Site 980 however appears relatively stable between H-events.

Our records indicate that a dominance of northern-sourced waters in the mid-depth northeast North Atlantic persisted throughout the last glacial period, but the absence of a strong influence of SSW at our intermediate depth study site does not preclude a dramatic slowdown of the deep ocean during certain H-events (Böhm et al., 2015). In fact, a shoaling of the overturning circulation cell is a feature common to many simulations of freshwater input to the North Atlantic where AMOC shutdown is incomplete (e.g. Flückiger et al., 2008).

5. Summary and Conclusions

We investigate the extent to which uncleaned foraminifera, fish debris and bulk sediment leachates can record regionally representative bottom water neodymium isotope compositions in the northeast North Atlantic by examining the isotopic signature of multiple substrates and associated rare earth element distributions. We find that neither local modification of bottom water chemistry by IRD labelling or redistribution of REE at depth within the sediment column exert a strong control over the REE and ϵ_{Nd} signatures preserved by planktonic foraminifera without their Fe-Mn oxide coatings removed at Site

980, making them suitable substrates for palaeoceanographic reconstructions. Foraminiferal and fish debris ϵ_{Nd} values show good agreement throughout the last 41,000 years, however, bulk sediment leachate values are offset towards more radiogenic values by 1–2 ϵ_{Nd} units throughout the Holocene, which we attribute to the increased influence of fine-grained radiogenic material transported by bottom currents on the sediment leachate values at this time. This result calls for careful evaluation of extracted leachate neodymium isotope compositions for leaching artifacts at North Atlantic drift sites.

By combining our new Nd isotope records with three additional proxies for water mass chemistry (B/Ca, $\delta^{13}\text{C}$ and $\delta^{18}\text{O}$ signatures of *C. wuellerstorfi*), we demonstrate that there is an increased influence of Nordic Seas overflow waters (and not southern-sourced waters) at 2.2 km depth in the Rockall Trough during the late glacial, possibly related in part to a reduction in LSW generation. A dominant presence of SSW at Site 980 at any time within the past 41 kyr is ruled out by reconstructed $[\text{CO}_3^{2-}]$ greater than 110 $\mu\text{mol/kg}$ throughout our record. We find that all four H-events within our study interval have different geochemical signatures, with H4 and H2 marked by ϵ_{Nd} excursions in opposing directions. Unradiogenic ϵ_{Nd} values and light oxygen and carbon isotope values during H4 could indicate an increased contribution of waters from either the Labrador Sea or deep waters forming south of the Greenland-Scotland Ridge, while the radiogenic ϵ_{Nd} signature recorded during H2 is more likely explained by an increased presence of overflow waters from the Nordic Seas.

We find that the stage of the glacial cycle occupied by H-events may not be the principle factor governing the response of the mid-depth North Atlantic to freshwater release. Instead, we suggest that this heterogeneity in the intermediate depth northeast

North Atlantic most likely arises due to differences in fresh water input locations, magnitudes and fluxes amongst H-events. The balance of contributions from different source regions to the northern intermediate/deep water endmember does not appear to remain constant, with important implications for the chemical signature of GNAIW that is transported downstream during millennial-scale climate events.

Acknowledgements

This research used samples provided by the Integrated Ocean Drilling (Discovery) Program IODP, which is sponsored by the US National Science Foundation and participating countries under management of Joint Oceanographic Institutions, Inc. We thank Walter Hale and Alex Wülbers for help with sampling, Kirsty Crocket for providing additional samples and Matt Cooper, Andy Milton, Mike Bolshaw and Dave Spanner for analytical support. Heiko Pälike, David Thornalley and Rachel Mills are thanked for productive discussions and comments on earlier versions of this work. We also thank three anonymous reviewers for their constructive feedback, which greatly improved the manuscript. Funding for this project was provided by NERC studentships to A.J.C. (grant NE/D005728/2) and T.B.C. (NE/I528626/1), with additional funding support from a Royal Society Wolfson Research Merit Award and NERC grants NE/F00141X/1 and NE/I006168/1 to P.A.W. and NE/D00876X/2 to G.L.F.

Competing financial interests

The authors declare no competing financial interests.

References

- Abbott, P.M., Davies, S.M., 2012. Volcanism and the Greenland ice-cores: the tephra record. *Earth-Science Reviews* 115, 173-191.
- Adkins, J.F., 2013. The role of deep ocean circulation in setting glacial climates. *Paleoceanography* 28, 539-561.
- Alley, R.B., Clark, P.U., Keigwin, L.D., Webb, R.S., 1999. Making sense of millennial-scale climate change. *Geophysical Monograph - American Geophysical Union* 112, 385-394.
- Andersen, K.K., Svensson, A., Johnsen, S.J., Rasmussen, S.O., Bigler, M., Röthlisberger, R., Ruth, U., Siggaard-Andersen, M.-L., Steffensen, J.P., Dahl-Jensen, D., Vinther, B.M., Clausen, H.B., 2006. The Greenland Ice Core Chronology 2005, 15-42 ka. Part 1: constructing the time scale. *Quaternary Science Reviews* 25, 3246-3257.
- Arsouze, T., Dutay, J.C., Lacan, F., Jeandel, C., 2009. Reconstructing the Nd oceanic cycle using a coupled dynamical-biogeochemical model. *Biogeosciences* 6, 2829-2846.
- Baas, J.H., Schönfeld, J., Zahn, R., 1998. Mid-depth oxygen drawdown during Heinrich events: evidence from benthic foraminiferal community structure, trace-fossil tiering, and benthic $\delta^{13}\text{C}$ at the Portuguese Margin. *Marine Geology* 152, 25-55.
- Bagniewski, W., Meissner, K.J., Menviel, L., Brennan, C.E., 2015. Quantification of factors impacting seawater and calcite $\delta^{18}\text{O}$ during Heinrich Stadials 1 and 4. *Paleoceanography* 30, 895-911.
- Ballini, M., Kissel, C., Colin, C., Richter, T., 2006. Deep-water mass source and dynamic associated with rapid climatic variations during the last glacial stage in the North

Atlantic: A multiproxy investigation of the detrital fraction of deep-sea sediments. *Geochem. Geophys. Geosyst.* 7, Q02N01.

Bard, E., 1988. Correction of Accelerator Mass Spectrometry ^{14}C Ages Measured in Planktonic Foraminifera: Paleoceanographic Implications. *Paleoceanography* 3, 635-645.

Bard, E., Arnold, M., Mangerud, J., Paterne, M., Labeyrie, L., Duprat, J., Mélières, M.-A., Sønstegaard, E., Duplessy, J.-C., 1994. The North Atlantic atmosphere-sea surface ^{14}C gradient during the Younger Dryas climatic event. *Earth and Planetary Science Letters* 126, 275-287.

Barker, S., Chen, J., Gong, X., Jonkers, L., Knorr, G., Thornalley, D., 2015. Icebergs not the trigger for North Atlantic cold events. *Nature* 520, 333-336.

Barker, S., Greaves, M., Elderfield, H., 2003. A study of cleaning procedures used for foraminiferal Mg/Ca paleothermometry. *Geochemistry, Geophysics, Geosystems* 4, 8407.

Bauch, D., Bauch, H.A., 2001. Last glacial benthic foraminiferal $\delta^{18}\text{O}$ anomalies in the polar North Atlantic: A modern analogue evaluation. *Journal of Geophysical Research: Oceans* 106, 9135-9143.

Bayon, G., German, C.R., Boella, R.M., Milton, J.A., Taylor, R.N., Nesbitt, R.W., 2002. An improved method for extracting marine sediment fractions and its application to Sr and Nd isotopic analysis. *Chemical Geology* 187, 179-199.

Benway, H.M., McManus, J.F., Oppo, D.W., Cullen, J.L., 2010. Hydrographic changes in the eastern subpolar North Atlantic during the last deglaciation. *Quaternary Science Reviews* 29, 3336-3345.

- Bertram, C.J., Elderfield, H., Shackleton, N.J., MacDonald, J.A., 1995. Cadmium/Calcium and Carbon Isotope Reconstructions of the Glacial Northeast Atlantic Ocean. *Paleoceanography* 10, 563-578.
- Bigg, G.R., Levine, R.C., Green, C.L., 2011. Modelling abrupt glacial North Atlantic freshening: Rates of change and their implications for Heinrich events. *Global and Planetary Change* 79, 176-192.
- Blaser, P., Lippold, J., Gutjahr, M., Frank, N., Link, J.M., Frank, M., 2016. Extracting foraminiferal Nd isotope signatures from bulk deep sea sediment by chemical leaching. *Chemical Geology* 439, 189–204.
- Böhm, E., Lippold, J., Gutjahr, M., Frank, M., Blaser, P., Antz, B., Fohlmeister, J., Frank, N., Andersen, M.B., Deininger, M., 2015. Strong and deep Atlantic meridional overturning circulation during the last glacial cycle. *Nature* 517, 73-76.
- Bond, G., Heinrich, H., Broecker, W., Labeyrie, L., McManus, J., Andrews, J., Huon, S., Jantschik, R., Clasen, S., Simet, C., 1992. Evidence for massive discharges of icebergs into the North Atlantic ocean during the last glacial period. *Nature* 360, 245-249.
- Bondevik, S., Mangerud, J., Birks, H.H., Gulliksen, S., Reimer, P., 2006. Changes in North Atlantic Radiocarbon Reservoir Ages During the Allerod and Younger Dryas. *Science* 312, 1514-1517.
- Boyle, E.A., Keigwin, L., 1987. North Atlantic thermohaline circulation during the past 20,000 years linked to high-latitude surface temperature. *Nature* 330, 35-40.
- Boyle, E.A., Keigwin, L.D., 1985. Comparison of Atlantic and Pacific paleochemical records for the last 215,000 years: changes in deep ocean circulation and chemical inventories. *Earth and Planetary Science Letters* 76, 135-150.

Bradt Miller, L.I., McManus, J.F., Robinson, L.F., 2014. $^{231}\text{Pa}/^{230}\text{Th}$ evidence for a weakened but persistent Atlantic meridional overturning circulation during Heinrich Stadial 1. *Nat Commun* 5, 5817.

Broecker, S.W., Peng, T.-H., 1982. *Tracers in the Sea*. Eldigio Press, Palisades, NY.

Broecker, W.S., Denton, G.H., 1989. The role of ocean-atmosphere reorganizations in glacial cycles. *Geochimica et Cosmochimica Acta* 53, 2465-2501.

Burckel, P., Waelbroeck, C., Gherardi, J.M., Pichat, S., Arz, H., Lippold, J., Dokken, T., Thil, F., 2015. Atlantic Ocean circulation changes preceded millennial tropical South America rainfall events during the last glacial. *Geophysical Research Letters* 42, 411-418.

Clark, C.D., Hughes, A.L.C., Greenwood, S.L., Jordan, C., Sejrup, H.P., 2012. Pattern and timing of retreat of the last British-Irish Ice Sheet. *Quaternary Science Reviews* 44, 112-146.

Cohen, A.S., O'Nions, R.K., Siegenthaler, R., Griffin, W.L., 1988. Chronology of the pressure-temperature history recorded by a granulite terrain. *Contributions to Mineralogy and Petrology* 98, 303-311.

Copard, K., Colin, C., Douville, E., Freiwald, A., Gudmundsson, G., De Mol, B., Frank, N., 2010. Nd isotopes in deep-sea corals in the North-eastern Atlantic. *Quaternary Science Reviews* 29, 2499-2508.

Cottet-Puinel, M., Weaver, A.J., Hillaire-Marcel, C., de Vernal, A., Clark, P.U., Eby, M., 2004. Variation of Labrador Sea Water formation over the Last Glacial cycle in a climate model of intermediate complexity. *Quaternary Science Reviews* 23, 449-465.

Crocker, A., 2014. Coupling of the Cryosphere and Ocean During Intervals of Rapid Climate Change in the Palaeo Record: A Multi-Proxy Study of the Heinrich Events of the Last Glacial from the Northeast Atlantic. PhD thesis, Department of Ocean and Earth Science. University of Southampton, p. 268.

Crocket, K.C., Vance, D., Gutjahr, M., Foster, G.L., Richards, D.A., 2011. Persistent Nordic deep-water overflow to the glacial North Atlantic. *Geology* 39, 515-518.

Curry, W.B., Oppo, D.W., 2005. Glacial water mass geometry and the distribution of $\delta^{13}\text{C}$ of ΣCO_2 in the western Atlantic Ocean. *Paleoceanography* 20, PA1017.

Darling, K.F., Kucera, M., Kroon, D., Wade, C.M., 2006. A resolution for the coiling direction paradox in *Neogloboquadrina pachyderma*. *Paleoceanography* 21, PA2011.

Davies, S.M., Abbott, P.M., Pearce, N.J.G., Wastegård, S., Blockley, S.P.E., 2012. Integrating the INTIMATE records using tephrochronology: rising to the challenge. *Quaternary Science Reviews* 36, 11-27.

de Baar, H.J.W., Bacon, M.P., Brewer, P.G., Bruland, K.W., 1985. Rare earth elements in the Pacific and Atlantic Oceans. *Geochimica et Cosmochimica Acta* 49, 1943-1959.

de Baar, H.J.W., German, C.R., Elderfield, H., van Gaans, P., 1988. Rare earth element distributions in anoxic waters of the Cariaco Trench. *Geochimica et Cosmochimica Acta* 52, 1203-1219.

de Vernal, A., Eynaud, F., Henry, M., Hillaire-Marcel, C., Londeix, L., Mangin, S., Matthiessen, J., Marret, F., Radi, T., Rochon, A., Solignac, S., Turon, J.L., 2005. Reconstruction of sea-surface conditions at middle to high latitudes of the Northern Hemisphere during the Last Glacial Maximum (LGM) based on dinoflagellate cyst assemblages. *Quaternary Science Reviews* 24, 897-924.

- Dokken, T.M., Jansen, E., 1999. Rapid changes in the mechanism of ocean convection during the last glacial period. *Nature* 401, 458-461.
- Dokken, T.M., Nisancioglu, K.H., Li, C., Battisti, D.S., Kissel, C., 2013. Dansgaard-Oeschger cycles: Interactions between ocean and sea ice intrinsic to the Nordic seas. *Paleoceanography* 28, 491-502.
- Duplessy, J.-C., Moyes, J., Pujol, C., 1980. Deep water formation in the North Atlantic Ocean during the last ice age. *Nature* 286, 479-482.
- Dyke, A.S., Andrews, J.T., Clark, P.U., England, J.H., Miller, G.H., Shaw, J., Veillette, J.J., 2002. The Laurentide and Innuitian ice sheets during the Last Glacial Maximum. *Quaternary Science Reviews* 21, 9-31.
- Elderfield, H., Greaves, M.J., 1982. The rare earth elements in seawater. *Nature* 296, 214-219.
- Elderfield, H., Whitfield, M., Burton, J.D., Bacon, M.P., Liss, P.S., 1988. The Oceanic Chemistry of the Rare-Earth Elements. *Philosophical Transactions of the Royal Society of London. Series A, Mathematical and Physical Sciences* 325, 105-126.
- Ellett, D.J., Martin, J.H.A., 1973. The physical and chemical oceanography of the Rockall channel. *Deep Sea Research and Oceanographic Abstracts* 20, 585-625.
- Elmore, A.C., Piotrowski, A.M., Wright, J.D., Scrivner, A.E., 2011. Testing the extraction of past seawater Nd isotopic composition from North Atlantic deep sea sediments and foraminifera. *Geochem. Geophys. Geosyst.* 12, Q09008.
- Eynaud, F., de Abreu, L., Voelker, A., Schönfeld, J., Salgueiro, E., Turon, J.-L., Penaud, A., Toucanne, S., Naughton, F., Sánchez Goñi, M.F., Malaizé, B., Cacho, I., 2009.

Position of the Polar Front along the western Iberian margin during key cold episodes of the last 45 ka. *Geochem. Geophys. Geosyst.* 10, Q07U05.

Eynaud, F., Zaragosi, S., Scourse, J.D., Mojtahid, M., Bourillet, J.F., Hall, I.R., Penaud, A., Locascio, M., Reijonen, A., 2007. Deglacial laminated facies on the NW European continental margin: The hydrographic significance of British-Irish Ice Sheet deglaciation and Fleuve Manche paleoriver discharges. *Geochem. Geophys. Geosyst.* 8, Q06019.

Flückiger, J., Knutti, R., White, J.C., Renssen, H., 2008. Modeled seasonality of glacial abrupt climate events. *Climate Dynamics* 31, 633-645.

Funder, S., Hansen, L., 1996. The Greenland ice sheet - a model for its culmination and decay during and after the last glacial maximum. *Bulletin of the Geological Society of Denmark* 42, 137-152.

Garrison, T., 2011. *Essentials of oceanography*. Thomson Brooks/Cole, Cengage Learning, Inc.

German, C.R., Elderfield, H., 1990. Application of the Ce anomaly as a paleoredox indicator: The ground rules. *Paleoceanography* 5, 823-833.

Gherardi, J.-M., Labeyrie, L., Nave, S., Francois, R., McManus, J.F., Cortijo, E., 2009. Glacial-interglacial circulation changes inferred from $^{231}\text{Pa}/^{230}\text{Th}$ sedimentary record in the North Atlantic region. *Paleoceanography* 24, PA2204.

Gierz, P., Lohmann, G., Wei, W., 2015. Response of Atlantic overturning to future warming in a coupled atmosphere-ocean-ice sheet model. *Geophysical Research Letters* 42, 6811-6818.

Goldberg, E.D., Koide, M., Schmitt, R.A., Smith, R.H., 1963. Rare-Earth distributions in the marine environment. *Journal of Geophysical Research* 68, 4209-4217.

Goldstein, S.L., O'Nions, R.K., Hamilton, P.J., 1984. A Sm-Nd isotopic study of atmospheric dusts and particulates from major river systems. *Earth and Planetary Science Letters* 70, 221-236.

Grandjean, P., Cappetta, H., Michard, A., Albarède, F., 1987. The assessment of REE patterns and $^{143}\text{Nd}/^{144}\text{Nd}$ ratios in fish remains. *Earth and Planetary Science Letters* 84, 181-196.

Grant, K.M., Rohling, E.J., Bar-Matthews, M., Ayalon, A., Medina-Elizalde, M., Ramsey, C.B., Satow, C., Roberts, A.P., 2012. Rapid coupling between ice volume and polar temperature over the past 150,000 years. *Nature* 491, 744-747.

Grousset, F.E., Biscaye, P.E., Revel, M., Petit, J.-R., Pye, K., Joussaume, S., Jouzel, J., 1992. Antarctic (Dome C) ice-core dust at 18 k.y. B.P.: Isotopic constraints on origins. *Earth and Planetary Science Letters* 111, 175-182.

Grousset, F.E., Labeyrie, L., Sinko, J.A., Cremer, M., Bond, G., Duprat, J., Cortijo, E., Huon, S., 1993. Patterns of Ice-Rafted Detritus in the Glacial North Atlantic (40-55°N). *Paleoceanography* 8, 175-192.

Gutjahr, M., Frank, M., Stirling, C.H., Klemm, V., van de Flierdt, T., Halliday, A.N., 2007. Reliable extraction of a deepwater trace metal isotope signal from Fe-Mn oxyhydroxide coatings of marine sediments. *Chemical Geology* 242, 351-370.

Gutjahr, M., Lippold, J., 2011. Early arrival of Southern Source Water in the deep North Atlantic prior to Heinrich event 2. *Paleoceanography* 26, PA2101.

Hall, I.R., Colmenero-Hidalgo, E., Zahn, R., Peck, V.L., Hemming, S.R., 2011. Centennial- to millennial-scale ice-ocean interactions in the subpolar northeast Atlantic 18-41 kyr ago. *Paleoceanography* 26, PA2224.

Hansen, B., Østerhus, S., 2000. North Atlantic-Nordic Seas exchanges. *Progress In Oceanography* 45, 109-208.

Heinrich, H., 1988. Origin and consequences of cyclic ice rafting in the Northeast Atlantic Ocean during the past 130,000 years. *Quaternary Research* 29, 142-152.

Hemming, S.R., 2004. Heinrich events: Massive late Pleistocene detritus layers of the North Atlantic and their global climate imprint. *Rev. Geophys.* 42, RG1005.

Hillaire-Marcel, C., de Vernal, A., 2008. Stable isotope clue to episodic sea ice formation in the glacial North Atlantic. *Earth and Planetary Science Letters* 268, 143-150.

Hillaire-Marcel, C., de Vernal, A., Candon, L., Bilodeau, G., Stoner, J., 2001. Changes of potential density gradients in the northwestern North Atlantic during the last climatic cycle based on a multiproxy approach, *The Oceans and Rapid Climate Change: Past, Present, and Future*. AGU, Washington, DC, pp. 83-100.

Hodell, D.A., Curtis, J.H., 2008. Oxygen and carbon isotopes of detrital carbonate in North Atlantic Heinrich Events. *Marine Geology* 256, 30-35.

Holser, W.T., 1997. Evaluation of the application of rare-earth elements to paleoceanography. *Palaeogeography, Palaeoclimatology, Palaeoecology* 132, 309-323.

Innocent, C., Fagel, N., Stevenson, R.K., Hillaire-Marcel, C., 1997. Sm-Nd signature of modern and late Quaternary sediments from the northwest North Atlantic: Implications for deep current changes since the Last Glacial Maximum. *Earth and Planetary Science Letters* 146, 607-625.

Jaccard, S.L., Galbraith, E.D., 2012. Large climate-driven changes of oceanic oxygen concentrations during the last deglaciation. *Nature Geosci* 5, 151-156.

Jacobsen, S.B., Wasserburg, G.J., 1980. Sm-Nd isotopic evolution of chondrites. *Earth and Planetary Science Letters* 50, 139-155.

Jansen, E., Fronval, T., Rack, F., Channell, J.E.T., 2000. Pliocene-Pleistocene Ice Rafting History and Cyclicity in the Nordic Seas During the Last 3.5 Myr. *Paleoceanography* 15, 709-721.

Jeandel, C., Arsouze, T., Lacan, F., Téchiné, P., Dutay, J.C., 2007. Isotopic Nd compositions and concentrations of the lithogenic inputs into the ocean: A compilation, with an emphasis on the margins. *Chemical Geology* 239, 156-164.

Johnson, C., Sherwin, T., Smythe-Wright, D., Shimmield, T., Turrell, W., 2010. Wyville Thomson Ridge Overflow Water: Spatial and temporal distribution in the Rockall Trough. *Deep Sea Research Part I: Oceanographic Research Papers* 57, 1153-1162.

Jones, C.E., Halliday, A.N., Rea, D.K., Owen, R.M., 1994. Neodymium isotopic variations in North Pacific modern silicate sediment and the insignificance of detrital REE contributions to seawater. *Earth and Planetary Science Letters* 127, 55-66.

Jonkers, L., Zahn, R., Thomas, A., Henderson, G., Abouchami, W., François, R., Masque, P., Hall, I.R., Bickert, T., 2015. Deep circulation changes in the central South Atlantic during the past 145 kyrs reflected in a combined $^{231}\text{Pa}/^{230}\text{Th}$, Neodymium isotope and benthic record. *Earth and Planetary Science Letters* 419, 14-21.

Keigwin, L.D., Jones, G.A., Lehman, S.J., Boyle, E.A., 1991. Deglacial meltwater discharge, North Atlantic Deep Circulation, and abrupt climate change. *Journal of Geophysical Research: Oceans* 96, 16811-16826.

Key, R.M., Kozyr, A., Sabine, C.L., Lee, K., Wanninkhof, R., Bullister, J.L., Feely, R.A., Millero, F.J., Mordy, C., Peng, T.H., 2004. A global ocean carbon climatology: Results

from Global Data Analysis Project (GLODAP). *Global Biogeochemical Cycles* 18, GB4031.

Kissel, C., 2005. Magnetic signature of rapid climatic variations in glacial North Atlantic, a review. *Comptes Rendus Geoscience* 337, 908-918.

Kissel, C., Laj, C., Labeyrie, L., Dokken, T., Voelker, A., Blamart, D., 1999. Rapid climatic variations during marine isotopic stage 3: magnetic analysis of sediments from Nordic Seas and North Atlantic. *Earth and Planetary Science Letters* 171, 489-502.

Labeyrie, L.D., Duplessy, J.-C., Duprat, J., Juillet-Leclerc, A., Moyes, J., Michel, E.,

Kallel, N., Shackleton, N.J., 1992. Changes in the vertical structure of the North Atlantic Ocean between glacial and modern times. *Quaternary Science Reviews* 11, 401-413.

Lacan, F., Jeandel, C., 2004a. Denmark Strait water circulation traced by heterogeneity in neodymium isotopic compositions. *Deep Sea Research Part I: Oceanographic Research Papers* 51, 71-82.

Lacan, F., Jeandel, C., 2004b. Neodymium isotopic composition and rare earth element concentrations in the deep and intermediate Nordic Seas: Constraints on the Iceland Scotland Overflow Water signature. *Geochem. Geophys. Geosyst.* 5, Q11006.

Lacan, F., Jeandel, C., 2004c. Subpolar Mode Water formation traced by neodymium isotopic composition. *Geophys. Res. Lett.* 31, L14306.

Lacan, F., Jeandel, C., 2005. Acquisition of the neodymium isotopic composition of the North Atlantic Deep Water. *Geochem. Geophys. Geosyst.* 6, Q12008.

Lacan, F., Tachikawa, K., Jeandel, C., 2012. Neodymium isotopic composition of the oceans: a compilation of seawater data. *Chemical Geology* 300-301, 177-184.

Lambelet, M., van de Flierdt, T., Crocket, K., Rehkämper, M., Kreissig, K., Coles, B., Rijkenberg, M.J.A., Gerringa, L.J.A., de Baar, H.J.W., Steinfeldt, R., 2016. Neodymium isotopic composition and concentration in the western North Atlantic Ocean: results from the GEOTRACES GA02 section. *Geochimica et Cosmochimica Acta* 177, 1–29.

Lang, D.C., Bailey, I., Wilson, P.A., Chalk, T.B., Foster, G.L., Gutjahr, M., 2016. Incursions of southern-sourced water into the deep North Atlantic during late Pliocene glacial intensification. *Nature Geosci* 9, 375-379.

Lekens, W.A.H., Sejrup, H.P., Haflidason, H., Knies, J., Richter, T., 2006. Meltwater and ice rafting in the southern Norwegian Sea between 20 and 40 calendar kyr B.P.: Implications for Fennoscandian Heinrich events. *Paleoceanography* 21, PA3013.

Lippold, J., Grützner, J., Winter, D., Lahaye, Y., Mangini, A., Christl, M., 2009. Does sedimentary $^{231}\text{Pa}/^{230}\text{Th}$ from the Bermuda Rise monitor past Atlantic Meridional Overturning Circulation? *Geophysical Research Letters* 36, L12601.

Lippold, J., Gutjahr, M., Blaser, P., Christner, E., de Carvalho Ferreira, M.L., Mulitza, S., Christl, M., Wombacher, F., Böhm, E., Antz, B., Cartapanis, O., Vogel, H., Jaccard, S.L., 2016. Deep water provenance and dynamics of the (de)glacial Atlantic meridional overturning circulation. *Earth and Planetary Science Letters* 445, 68-78.

Lowe, J.J., Rasmussen, S.O., Björck, S., Hoek, W.Z., Steffensen, J.P., Walker, M.J.C., Yu, Z.C., 2008. Synchronisation of palaeoenvironmental events in the North Atlantic region during the Last Termination: a revised protocol recommended by the INTIMATE group. *Quaternary Science Reviews* 27, 6-17.

Lynch-Stieglitz, J., Schmidt, M.W., Gene Henry, L., Curry, W.B., Skinner, L.C., Mulitza, S., Zhang, R., Chang, P., 2014. Muted change in Atlantic overturning circulation over some glacial-aged Heinrich events. *Nature Geosci* 7, 144-150.

Mackensen, A., Hubberten, H.W., Bickert, T., Fischer, G., Fütterer, D.K., 1993. The $\delta^{13}\text{C}$ in benthic foraminiferal tests of *Fontbotia wuellerstorfi* (Schwager) Relative to the $\delta^{13}\text{C}$ of dissolved inorganic carbon in Southern Ocean Deep Water: Implications for glacial ocean circulation models. *Paleoceanography* 8, 587-610.

MacLeod, K.G., Irving, A.J., 1996. Correlation of cerium anomalies with indicators of paleoenvironment. *Journal of Sedimentary Research* 66, 948-955.

Manighetti, B., McCave, I.N., 1995. Late Glacial and Holocene Palaeocurrents Around Rockall Bank, NE Atlantic Ocean. *Paleoceanography* 10, 611-626.

Martin, E.E., Blair, S.W., Kamenov, G.D., Scher, H.D., Bourbon, E., Basak, C., Newkirk, D.N., 2010. Extraction of Nd isotopes from bulk deep sea sediments for paleoceanographic studies on Cenozoic time scales. *Chemical Geology* 269, 414-431.

Martin, E.E., Haley, B.A., 2000. Fossil fish teeth as proxies for seawater Sr and Nd isotopes. *Geochimica et Cosmochimica Acta* 64, 835-847.

Martin, E.E., Scher, H.D., 2004. Preservation of seawater Sr and Nd isotopes in fossil fish teeth: bad news and good news. *Earth and Planetary Science Letters* 220, 25-39.

Maslin, M.A., Shackleton, N.J., Pflaumann, U., 1995. Surface Water Temperature, Salinity, and Density Changes in the Northeast Atlantic During the Last 45,000 Years: Heinrich Events, Deep Water Formation, and Climatic Rebounds. *Paleoceanography* 10, 527-544.

- McCartney, M.S., 1992. Recirculating components to the deep boundary current of the northern North Atlantic. *Progress In Oceanography* 29, 283-383.
- McCave, I.N., Manighetti, B., Beveridge, N.A.S., 1995a. Circulation in the glacial North Atlantic inferred from grain-size measurements. *Nature* 374, 149-152.
- McCave, I.N., Manighetti, B., Robinson, S.G., 1995b. Sortable silt and fine sediment size/composition slicing: Parameters for palaeocurrent speed and palaeoceanography. *Paleoceanography* 10, 593-610.
- McGrath, T., Nolan, G., McGovern, E., 2012. Chemical characteristics of water masses in the Rockall Trough. *Deep Sea Research Part I: Oceanographic Research Papers*.
- McIntyre, K.L., Howe, J.A., 2009. Bottom-current variability during the last glacial-deglacial transition, Northern Rockall Trough and Faroe Bank Channel, NE Atlantic. *Scottish Journal of Geology* 45, 43-57.
- McLennan, S.M., 1989. Rare earth elements in sedimentary rocks; influence of provenance and sedimentary processes. *Reviews in Mineralogy and Geochemistry* 21, 169-200.
- McManus, J.F., Francois, R., Gherardi, J.M., Keigwin, L.D., Brown-Leger, S., 2004. Collapse and rapid resumption of Atlantic meridional circulation linked to deglacial climate changes. *Nature* 428, 834-837.
- McManus, J.F., Oppo, D.W., Cullen, J.L., 1999. A 0.5-Million-Year Record of Millennial-Scale Climate Variability in the North Atlantic. *Science* 283, 971-975.
- Mearns, E.W., 1988. A samarium-neodymium isotopic survey of modern river sediments from Northern Britain. *Chemical Geology: Isotope Geoscience section* 73, 1-13.

Meland, M.Y., Dokken, T.M., Jansen, E., Hevrøy, K., 2008. Water mass properties and exchange between the Nordic seas and the northern North Atlantic during the period 23-6 ka: Benthic oxygen isotopic evidence. *Paleoceanography* 23, PA1210.

Mulitza, S., Prange, M., Stuut, J.-B., Zabel, M., von Dobeneck, T., Itambi, A.C., Nizou, J., Schulz, M., Wefer, G., 2008. Sahel megadroughts triggered by glacial slowdowns of Atlantic meridional overturning. *Paleoceanography* 23, PA4206.

New, A.L., Smythe-Wright, D., 2001. Aspects of the circulation in the Rockall Trough. *Continental Shelf Research* 21, 777-810.

North Greenland Ice Core Project Members, Andersen, K.K., Azuma, N., Barnola, J.-M., Bigler, M., Biscaye, P., Caillon, N., Chappellaz, J., Clausen, H.B., Dahl-Jensen, D., Fischer, H., Flückiger, J., Fritzsche, D., Fujii, Y., Goto-Azuma, K., Grønvold, K., Gundestrup, N.S., Hansson, M., Huber, C., Hvidberg, C.S., Johnsen, S.J., Jonsell, U., Jouzel, J., Kipfstuhl, S., Landais, A., Leuenberger, M., Lorrain, R., Masson-Delmotte, V., Miller, H., Motoyama, H., Narita, H., Popp, T., Rasmussen, S.O., Raynaud, D., Rothlisberger, R., Ruth, U., Samyn, D., Schwander, J., Shoji, H., Siggard-Andersen, M.-L., Steffensen, J.P., Stocker, T., Sveinbjörnsdóttir, A.E., Svensson, A., Takata, M., Tison, J.-L., Thorsteinsson, T., Watanabe, O., Wilhelms, F., White, J.W.C., 2004. High-resolution record of Northern Hemisphere climate extending into the last interglacial period. *Nature* 431, 147-151.

Nuttin, L., Maccali, J., Hillaire-Marcel, C., 2015. U, Th and Pa insights into sedimentological and paleoceanographic changes off Hudson Strait (Labrador Sea) during the last ~ 37 ka with special attention to methodological issues. *Quaternary Science Reviews* 115, 39-49.

O'Nions, R.K., Carter, S.R., Cohen, R.S., Evensen, N.M., Hamilton, P.J., 1978. Pb, Nd and Sr isotopes in oceanic ferromanganese deposits and ocean floor basalts. *Nature* 273, 435-438.

Olsen, A., Ninnemann, U., 2010. Large $\delta^{13}\text{C}$ Gradients in the Preindustrial North Atlantic Revealed. *Science* 330, 658-659.

Oppo, D.W., Lehman, S.J., 1993. Mid-Depth Circulation of the Subpolar North Atlantic During the Last Glacial Maximum. *Science* 259, 1148-1152.

Oppo, D.W., McManus, J.F., Cullen, J.L., 2003. Palaeo-oceanography: Deepwater variability in the Holocene epoch. *Nature* 422, 277-277.

Oppo, D.W., McManus, J.F., Cullen, J.L., 2006. Evolution and demise of the Last Interglacial warmth in the subpolar North Atlantic. *Quaternary Science Reviews* 25, 3268-3277.

Otto-Bliesner, B.L., Brady, E.C., 2010. The sensitivity of the climate response to the magnitude and location of freshwater forcing: last glacial maximum experiments. *Quaternary Science Reviews* 29, 56-73.

Paillard, D., Labeyrie, L., Yiou, P., 1996. Macintosh program performs time-series analysis. *Eos. Trans. AGU* 77.

Palmer, M.R., Elderfield, H., 1985. Variations in the Nd isotopic composition of foraminifera from Atlantic Ocean sediments. *Earth and Planetary Science Letters* 73, 299-305.

Peck, V.L., Hall, I.R., Zahn, R., Grousset, F., Hemming, S.R., Scourse, J.D., 2007. The relationship of Heinrich events and their European precursors over the past 60 ka BP: a

multi-proxy ice-rafted debris provenance study in the North East Atlantic. *Quaternary Science Reviews* 26, 862-875.

Piepgas, D.J., Wasserburg, G.J., Dasch, E.J., 1979. The isotopic composition of Nd in different ocean masses. *Earth and Planetary Science Letters* 45, 223-236.

Pin, C., Zalduegui, J.S., 1997. Sequential separation of light rare-earth elements, thorium and uranium by miniaturized extraction chromatography: Application to isotopic analyses of silicate rocks. *Analytica Chimica Acta* 339, 79-89.

Piotrowski, A.M., Galy, A., Nicholl, J.A.L., Roberts, N., Wilson, D.J., Clegg, J.A., Yu, J., 2012. Reconstructing deglacial North and South Atlantic deep water sourcing using foraminiferal Nd isotopes. *Earth and Planetary Science Letters* 357-358, 289-297.

Piotrowski, A.M., Goldstein, S.L., Hemming, S.R., Fairbanks, R.G., 2004. Intensification and variability of ocean thermohaline circulation through the last deglaciation. *Earth and Planetary Science Letters* 225, 205-220.

Piotrowski, A.M., Goldstein, S.L., Hemming, S.R., Fairbanks, R.G., 2005. Temporal Relationships of Carbon Cycling and Ocean Circulation at Glacial Boundaries. *Science* 307, 1933-1938.

Piotrowski, A.M., Goldstein, S.L., Hemming, S.R., Fairbanks, R.G., Zylberberg, D.R., 2008. Oscillating glacial northern and southern deep water formation from combined neodymium and carbon isotopes. *Earth and Planetary Science Letters* 272, 394-405.

Rae, J.W.B., Foster, G.L., Schmidt, D.N., Elliott, T., 2011. Boron isotopes and B/Ca in benthic foraminifera: Proxies for the deep ocean carbonate system. *Earth and Planetary Science Letters* 302, 403-413.

Rahmstorf, S., 2002. Ocean circulation and climate during the past 120,000 years. *Nature* 419, 207-214.

Rasmussen, S.O., Andersen, K.K., Svensson, A.M., Steffensen, J.P., Vinther, B.M., Clausen, H.B., Siggaard-Andersen, M.L., Johnsen, S.J., Larsen, L.B., Dahl-Jensen, D., Bigler, M., Röthlisberger, R., Fischer, H., Goto-Azuma, K., Hansson, M.E., Ruth, U., 2006. A new Greenland ice core chronology for the last glacial termination. *J. Geophys. Res.* 111, D06102.

Rasmussen, T.L., Thomsen, E., 2009. Stable isotope signals from brines in the Barents Sea: Implications for brine formation during the last glaciation. *Geology* 37, 903-906.

Reimer, P.J., Bard, E., Bayliss, A., Beck, J.W., Blackwell, P.G., Bronk Ramsey, C., Buck, C.E., Cheng, H., Edwards, R.L., Friedrich, M., Grootes, P.M., Guilderson, T.P., Haflidason, H., Hajdas, I., Hatté, C., Heaton, T.J., Hoffmann, D.L., Hogg, A.G., Hughen, K.A., Kaiser, K.F., Kromer, B., Manning, S.W., Niu, M., Reimer, R.W., Richards, D.A., Scott, E.M., Southon, J.R., Staff, R.A., Turney, C.S.M., van der Plicht, J., 2013. IntCal13 and Marine13 Radiocarbon Age Calibration Curves 0–50,000 Years cal BP.

Reynard, B., Lécuyer, C., Grandjean, P., 1999. Crystal-chemical controls on rare-earth element concentrations in fossil biogenic apatites and implications for paleoenvironmental reconstructions. *Chemical Geology* 155, 233-241.

Rickli, J., Gutjahr, M., Vance, D., Fischer-Gödde, M., Hillenbrand, C.-D., Kuhn, G., 2014. Neodymium and hafnium boundary contributions to seawater along the West Antarctic continental margin. *Earth and Planetary Science Letters* 394, 99-110.

Roberts, N.L., Piotrowski, A.M., 2015. Radiogenic Nd isotope labeling of the northern NE Atlantic during MIS 2. *Earth and Planetary Science Letters* 423, 125-133.

Roberts, N.L., Piotrowski, A.M., Elderfield, H., Eglinton, T.I., Lomas, M.W., 2012. Rare earth element association with foraminifera. *Geochimica et Cosmochimica Acta* 94, 57-71.

Roberts, N.L., Piotrowski, A.M., McManus, J.F., Keigwin, L.D., 2010. Synchronous Deglacial Overturning and Water Mass Source Changes. *Science* 327, 75-78.

Robinson, L.F., Adkins, J.F., Keigwin, L.D., Southon, J., Fernandez, D.P., Wang, S.L., Scheirer, D.S., 2005. Radiocarbon Variability in the Western North Atlantic During the Last Deglaciation. *Science* 310, 1469-1473.

Rogerson, M., Rohling, E.J., Weaver, P.P.E., Murray, J.W.C., 2005. Glacial to interglacial changes in the settling depth of the Mediterranean Outflow plume. *Paleoceanography* 20, PA3007.

Ruddiman, W.F., 1977. Late Quaternary deposition of ice-rafted sand in the subpolar North Atlantic (lat 40° to 65°N). *Geological Society of America Bulletin* 88, 1813-1827.

Rutberg, R.L., Hemming, S.R., Goldstein, S.L., 2000. Reduced North Atlantic Deep Water flux to the glacial Southern Ocean inferred from neodymium isotope ratios. *Nature* 405, 935-938.

Sarbas, B., Nohl, U., 2008. The GEOROC database as part of a growing geoinformatics network, 2008 Geoinformatics conference.

Sarmiento, J.L., Gruber, N., 2004. *Ocean Biogeochemical Dynamics*. Princeton University Press, Princeton, NJ.

Sarnthein, M., Winn, K., Jung, S.J.A., Duplessy, J.-C., Labeyrie, L., Erlenkeuser, H., Ganssen, G., 1994. Changes in East Atlantic Deepwater Circulation Over the Last 30,000 years: Eight Time Slice Reconstructions. *Paleoceanography* 9, 209-267.

- Schönfeld, J., Zahn, R., de Abreu, L., 2003. Surface and deep water response to rapid climate changes at the Western Iberian Margin. *Global and Planetary Change* 36, 237-264.
- Sejrup, H.P., Hjelstuen, B.O., Torbjørn Dahlgren, K.I., Haflidason, H., Kuijpers, A., Nygård, A., Praeg, D., Stoker, M.S., Vorren, T.O., 2005. Pleistocene glacial history of the NW European continental margin. *Marine and Petroleum Geology* 22, 1111-1129.
- Shackleton, N.J., Opdyke, N.D., 1973. Oxygen isotope and palaeomagnetic stratigraphy of Equatorial Pacific core V28-238: Oxygen isotope temperatures and ice volumes on a 10^5 year and 10^6 year scale. *Quaternary Research* 3, 39-55.
- Shipboard Scientific Party, 1996. Sites 980/981, in: Jansen, E., Raymo, M.E., Blum P. et al. (Eds.), *Proceedings of the Ocean Drilling Program, Initial Reports*. College station, TX, pp. 49-90.
- Sholkovitz, E.R., 1988. Rare earth elements in the sediments of the North Atlantic Ocean, Amazon Delta, and East China Sea; reinterpretation of terrigenous input patterns to the oceans. *American Journal of Science* 288, 236-281.
- Siddall, M., Rohling, E.J., Almogi-Labin, A., Hemleben, C., Meischner, D., Schmelzer, I., Smeed, D.A., 2003. Sea-level fluctuations during the last glacial cycle. *Nature* 423, 853-858.
- Sigman, D.M., Boyle, E.A., 2000. Glacial/interglacial variations in atmospheric carbon dioxide. *Nature* 407, 859-869.
- Sigman, D.M., Hain, M.P., Haug, G.H., 2010. The polar ocean and glacial cycles in atmospheric CO₂ concentration. *Nature* 466, 47-55.

Singarayer, J.S., Valdes, P.J., 2010. High-latitude climate sensitivity to ice-sheet forcing over the last 120 kyr. *Quaternary Science Reviews* 29, 43-55.

Smith, R.S., Gregory, J.M., 2009. A study of the sensitivity of ocean overturning circulation and climate to freshwater input in different regions of the North Atlantic. *Geophysical Research Letters* 36, L15701.

Snoeckx, H., Grousset, F., Revel, M., Boelaert, A., 1999. European contribution of ice-rafted sand to Heinrich layers H3 and H4. *Marine Geology* 158, 197-208.

Spivack, A.J., Wasserburg, G.J., 1988. Neodymium isotopic composition of the Mediterranean outflow and the eastern North Atlantic. *Geochimica et Cosmochimica Acta* 52, 2767-2773.

Stanford, J.D., Rohling, E.J., Bacon, S., Roberts, A.P., Grousset, F.E., Bolshaw, M., 2011. A new concept for the paleoceanographic evolution of Heinrich event 1 in the North Atlantic. *Quaternary Science Reviews* 30, 1047-1066.

Staudigel, H., Doyle, P., Zindler, A., 1985. Sr and Nd isotope systematics in fish teeth. *Earth and Planetary Science Letters* 76, 45-56.

Stern, J.V., Lisiecki, L.E., 2013. North Atlantic circulation and reservoir age changes over the past 41,000 years. *Geophysical Research Letters* 40, 3693-3697.

Stichel, T., Frank, M., Rickli, J., Haley, B.A., 2012. The hafnium and neodymium isotope composition of seawater in the Atlantic sector of the Southern Ocean. *Earth and Planetary Science Letters* 317–318, 282-294.

Stille, P., 1992. Nd-Sr isotope evidence for dramatic changes of paleocurrents in the Atlantic Ocean during the past 80 m.y. *Geology* 20, 387-390.

- Stille, P., Fischer, H., 1990. Secular variation in the isotopic composition of Nd in Tethys seawater. *Geochimica et Cosmochimica Acta* 54, 3139-3145.
- Stuiver, M., Reimer, P.J., 1993. Extended ^{14}C database and revised CALIB radiocarbon calibration program. *Radiocarbon* 35, 215-230.
- Stuiver, M., Reimer, P.J., Reimer, R.W., 2005. CALIB 5.0.
- Svensson, A., Andersen, K.K., Bigler, M., Clausen, H.B., Dahl-Jensen, D., Davies, S.M., Johnsen, S.J., Muscheler, R., Parrenin, F., Rasmussen, S.O., Röthlisberger, R., Seierstad, I., Steffensen, J.P., Vinther, B.M., 2008. A 60 000 year Greenland stratigraphic ice core chronology. *Clim. Past* 4, 47-57.
- Swingedouw, D., Mignot, J., Braconnot, P., Mosquet, E., Kageyama, M., Alkama, R., 2009. Impact of Freshwater Release in the North Atlantic under Different Climate Conditions in an OAGCM. *Journal of Climate* 22, 6377-6403.
- Tachikawa, K., Athias, V., Jeandel, C., 2003. Neodymium budget in the modern ocean and paleo-oceanographic implications. *J. Geophys. Res.* 108, 3254.
- Tachikawa, K., Jeandel, C., Roy-Barman, M., 1999. A new approach to the Nd residence time in the ocean: the role of atmospheric inputs. *Earth and Planetary Science Letters* 170, 433-446.
- Tachikawa, K., Piotrowski, A.M., Bayon, G., 2014. Neodymium associated with foraminiferal carbonate as a recorder of seawater isotopic signatures. *Quaternary Science Reviews* 88, 1-13.
- Tanaka, T., Togashi, S., Kamioka, H., Amakawa, H., Kagami, H., Hamamoto, T., Yuhara, M., Orihashi, Y., Yoneda, S., Shimizu, H., Kunimaru, T., Takahashi, K., Yanagi, T., Nakano, T., Fujimaki, H., Shinjo, R., Asahara, Y., Tanimizu, M., Dragusanu, C.,

2000. JNdi-1: a neodymium isotopic reference in consistency with LaJolla neodymium.

Chemical Geology 168, 279-281.

Taylor, S.R., McLennan, S.M., 1985. *The continental crust: its composition and evolution*. Blackwell, Oxford.

Thornalley, D.J.R., Barker, S., Becker, J., Hall, I.R., Knorr, G., 2013. Abrupt changes in deep Atlantic circulation during the transition to full glacial conditions.

Paleoceanography 28, 253-262.

Thornalley, D.J.R., Bauch, H.A., Gebbie, G., Guo, W., Ziegler, M., Bernasconi, S.M., Barker, S., Skinner, L.C., Yu, J., 2015. A warm and poorly ventilated deep Arctic Mediterranean during the last glacial period. *Science* 349, 706-710.

Thornalley, D.J.R., Elderfield, H., McCave, I.N., 2010. Intermediate and deep water paleoceanography of the northern North Atlantic over the past 21,000 years.

Paleoceanography 25, PA1211.

Toucanne, S., Zaragosi, S., Bourillet, J.F., Cremer, M., Eynaud, F., Van Vliet-Lanoë, B., Penaud, A., Fontanier, C., Turon, J.L., Cortijo, E., Gibbard, P.L., 2009. Timing of massive 'Fleuve Manche' discharges over the last 350 kyr: insights into the European ice-sheet oscillations and the European drainage network from MIS 10 to 2. *Quaternary Science Reviews* 28, 1238-1256.

van de Flierdt, T., Robinson, L.F., Adkins, J.F., Hemming, S.R., Goldstein, S.L., 2006.

Temporal stability of the neodymium isotope signature of the Holocene to glacial North Atlantic. *Paleoceanography* 21, PA4102.

van Kreveld, S.A., 1996. Northeast Atlantic Late Quaternary planktic Foraminifera as primary productivity and water mass indicators. *Scripta Geologica* 113, 23-91.

Vance, D., Thirlwall, M., 2002. An assessment of mass discrimination in MC-ICPMS using Nd isotopes. *Chemical Geology* 185, 227-240.

Vaughan, D.G., Comiso, J.C., Allison, I., Carrasco, J., Kaser, G., Kwok, R., Mote, P., Murray, T., Paul, F., Ren, J., Rignot, E., Solomina, O., Steffen, K., Zhang, T., 2013. Observations: Cryosphere, in: Stocker, T.F., Qin, D., Plattner, G.-K., Tignor, M., Allen, S.K., Boschung, J., Nauels, A., Xia, Y., Bex, V., Midgley, P.M. (Eds.), *Climate Change 2013: The Physical Science Basis. Contribution of Working Group I to the Fifth Assessment Report of the Intergovernmental Panel on Climate Change*. Cambridge University Press, Cambridge, United Kingdom and New York, NY, USA.

Vidal, L., Labeyrie, L., Cortijo, E., Arnold, M., Duplessy, J.C., Michel, E., Becqué, S., van Weering, T.C.E., 1997. Evidence for changes in the North Atlantic Deep Water linked to meltwater surges during the Heinrich events. *Earth and Planetary Science Letters* 146, 13-27.

Vidal, L., Labeyrie, L., van Weering, T.C.E., 1998. Benthic $\delta^{18}\text{O}$ Records in the North Atlantic Over the Last Glacial Period (60-10 kyr): Evidence for Brine Formation. *Paleoceanography* 13, 245-251.

Vinther, B.M., Clausen, H.B., Johnsen, S.J., Rasmussen, S.O., Andersen, K.K., Buchardt, S.L., Dahl-Jensen, D., Seierstad, I.K., Siggaard-Andersen, M.L., Steffensen, J.P., Svensson, A., Olsen, J., Heinemeier, J., 2006. A synchronized dating of three Greenland ice cores throughout the Holocene. *J. Geophys. Res.* 111, D13102.

Voelker, A.H.L., Lebreiro, S.M., Schönfeld, J., Cacho, I., Erlenkeuser, H., Abrantes, F., 2006. Mediterranean outflow strengthening during northern hemisphere coolings: A salt source for the glacial Atlantic? *Earth and Planetary Science Letters* 245, 39-55.

Waelbroeck, C., Duplessy, J.-C., Michel, E., Labeyrie, L., Paillard, D., Duprat, J., 2001. The timing of the last deglaciation in North Atlantic climate records. *Nature* 412, 724-727.

Weber, M.E., Mayer, L.A., Hillaire-Marcel, C., Bilodeau, G., Rack, F., Hiscott, R.N., Aksu, A.E., 2001. Derivation of $\delta^{18}\text{O}$ from Sediment Core Log Data: Implications for Millennial-Scale Climate Change in the Labrador Sea. *Paleoceanography* 16, 503-514.

Wei, R., Abouchami, W., Zahn, R., Masque, P., 2015. Deep circulation changes in the South Atlantic since the Last Glacial Maximum from Nd isotope and multi-proxy records. *Earth and Planetary Science Letters* 434, 18-29.

Wilson, D.J., Crocket, K.C., van de Flierdt, T., Robinson, L.F., Adkins, J.F., 2014. Dynamic intermediate ocean circulation in the North Atlantic during Heinrich Stadial 1: A radiocarbon and neodymium isotope perspective. *Paleoceanography*, 2014PA002674.

Wilson, D.J., Piotrowski, A.M., Galy, A., Banakar, V.K., 2015. Interhemispheric controls on deep ocean circulation and carbon chemistry during the last two glacial cycles. *Paleoceanography* 30, 621-641.

Wilson, D.J., Piotrowski, A.M., Galy, A., Clegg, J.A., 2013. Reactivity of neodymium carriers in deep sea sediments: implications for boundary exchange and paleoceanography. *Geochimica et Cosmochimica Acta* 109, 197-221.

Wilson, D.J., Piotrowski, A.M., Galy, A., McCave, I.N., 2012. A boundary exchange influence on deglacial neodymium isotope records from the deep western Indian Ocean. *Earth and Planetary Science Letters* 341–344, 35-47.

Yu, E.-F., Francois, R., Bacon, M.P., 1996. Similar rates of modern and last-glacial ocean thermohaline circulation inferred from radiochemical data. *Nature* 379, 689-694.

- Yu, J., Anderson, R.F., Jin, Z., Menviel, L., Zhang, F., Ryerson, F.J., Rohling, E.J., 2014. Deep South Atlantic carbonate chemistry and increased interocean deep water exchange during last deglaciation. *Quaternary Science Reviews* 90, 80-89.
- Yu, J., Elderfield, H., 2007. Benthic foraminiferal B/Ca ratios reflect deep water carbonate saturation state. *Earth and Planetary Science Letters* 258, 73-86.
- Yu, J., Elderfield, H., Piotrowski, A.M., 2008. Seawater carbonate ion- $\delta^{13}\text{C}$ systematics and application to glacial-interglacial North Atlantic ocean circulation. *Earth and Planetary Science Letters* 271, 209-220.
- Zahn, R., Schönfeld, J., Kudrass, H.-R., Park, M.-H., Erlenkeuser, H., Grootes, P., 1997. Thermohaline Instability in the North Atlantic During Meltwater Events: Stable Isotope and Ice-Rafted Detritus Records from Core SO75-26KL, Portuguese Margin. *Paleoceanography* 12, 696-710.

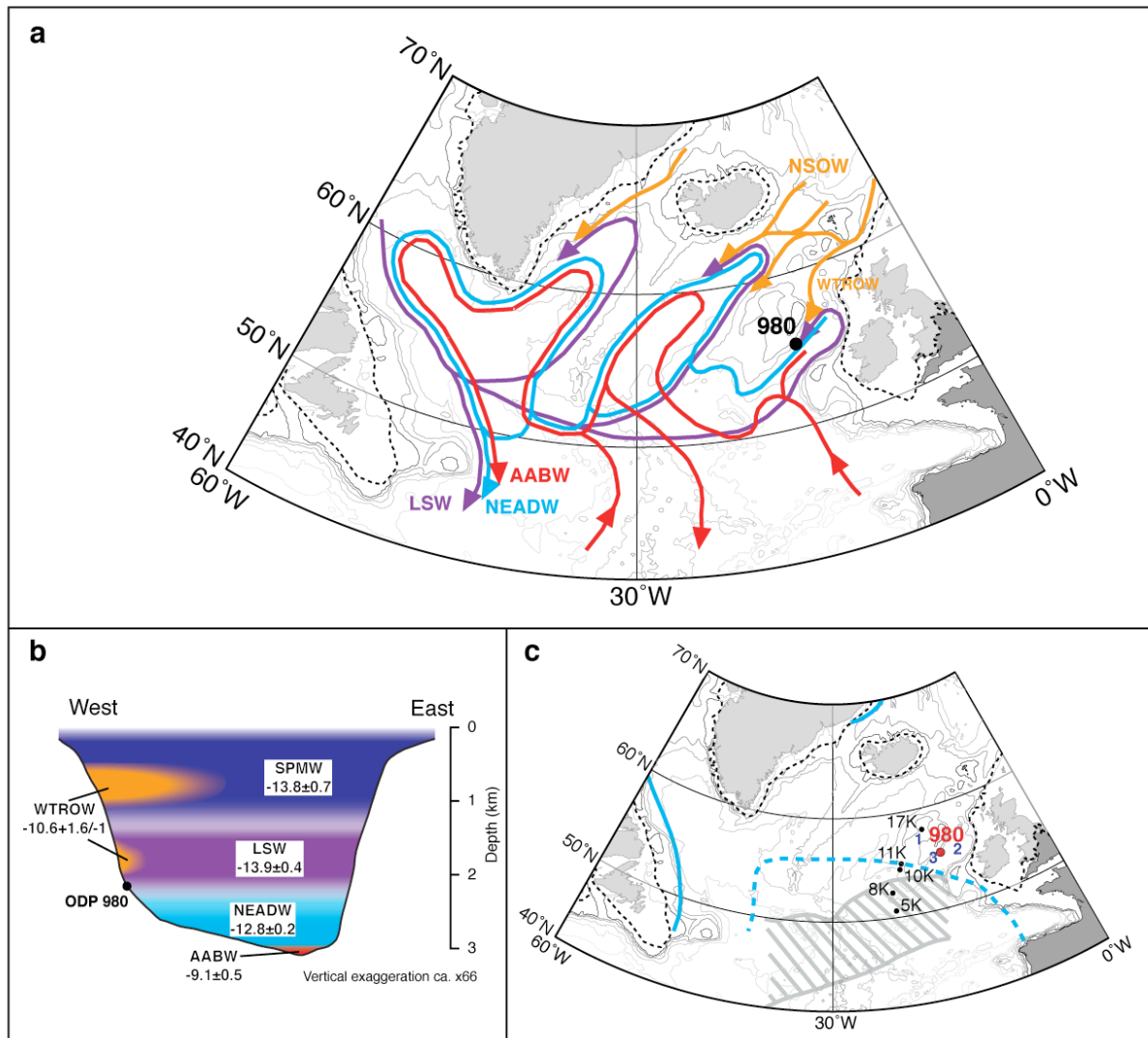


Fig. 1: (a) The North Atlantic region showing the location of the main study site (ODP Site 980, in black). Dotted lines mark the approximate maximum spatial extent of continental ice sheets during the last glacial maximum (Clark et al., 2012; Dyke et al., 2002; Funder and Hansen, 1996; Sejrup et al., 2005). Arrows represent modern major intermediate and deep current pathways with Nordic Sea overflows (NSOW, orange, also includes Wyville-Thomson Ridge overflow waters or WTROW), Labrador Sea Water (LSW, purple), Northeast Atlantic Deep Water (NEADW, light blue) and Antarctic Bottom Water (AABW, red), based upon McCartney (1992), Hansen and Østerhus (2000), New and Smythe-Wright (2001) and Lacan and Jeandel (2005). (b) Schematic cross-section of the major water masses in the modern Rockall Trough, based upon McGrath et

al. (2012) and Johnson et al. (2010). Colours as panel (a), with the addition of Subpolar Mode Water (SPMW, dark blue). Numbers give neodymium isotope signature of water masses today (Crocker, 2014; Crocket et al., 2011; Lacan and Jeandel, 2004c; Lacan and Jeandel, 2005; Lacan et al., 2012; Stichel et al., 2012). Note that the ϵ_{Nd} value of AABW shown is the AABW endmember recorded in the Atlantic section of the Southern Ocean; this value is likely modified by mixing and boundary exchange as the water mass moves northwards (e.g. Lambelet et al., 2016). (c) North Atlantic region showing the location of the main study site (ODP Site 980, in red) and BOFS sites referred to in the text (black). Grey stripes indicate the main belt of ice-rafted debris deposition in the glacial north Atlantic during the Last Glacial Maximum (Ruddiman, 1977). Dark blue numbers: 1 – Rockall Plateau, 2 – Rockall Trough, 3 – Feni Drift. Last Glacial Maximum limit of perennial sea ice indicated by solid light blue line with dashed light blue line marking extreme limit of winter sea ice (de Vernal et al., 2005; Hillaire-Marcel and de Vernal, 2008).

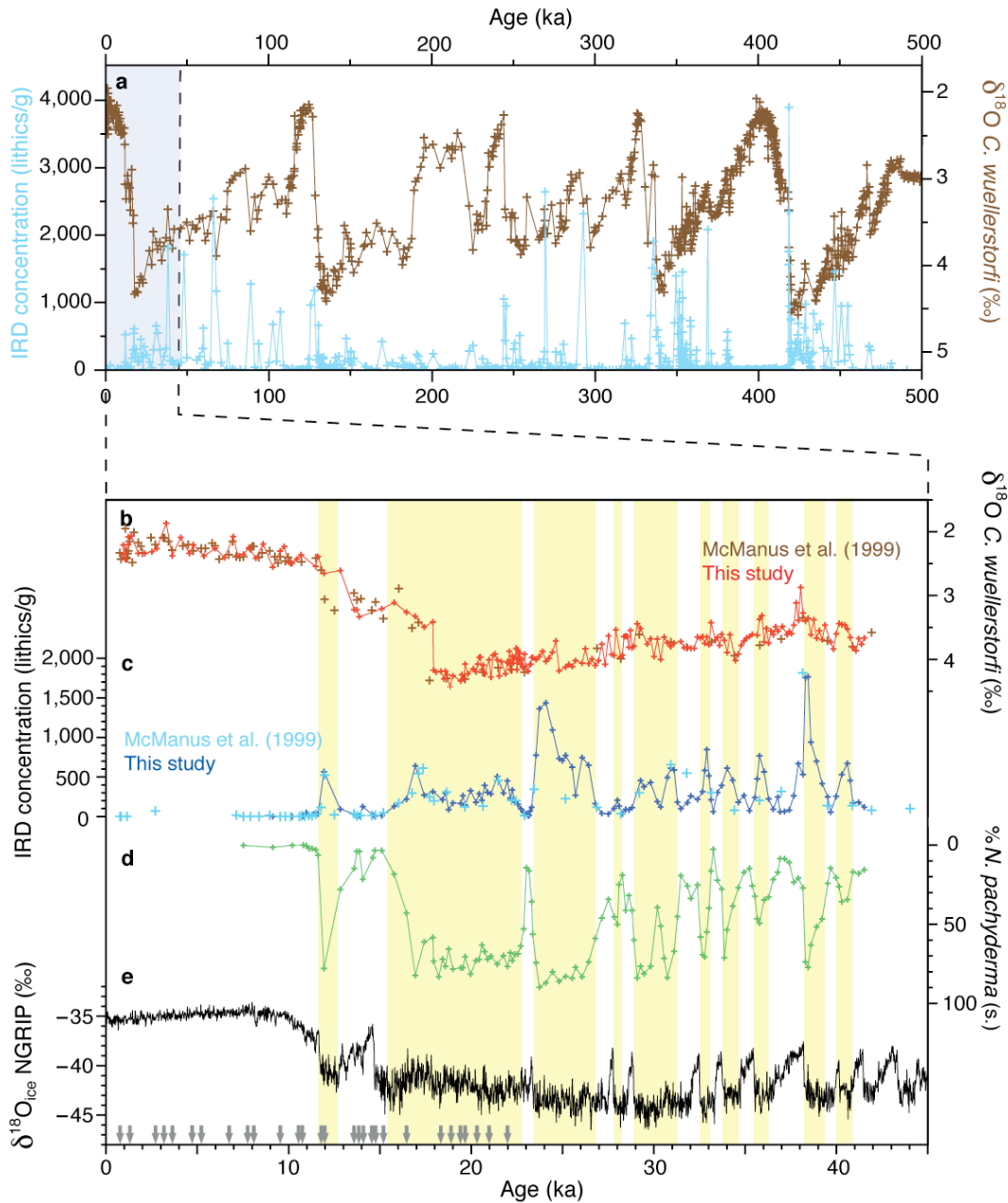


Fig. 2: Suborbital variability at ODP Site 980. (a) Data set of McManus et al. (1999), benthic foraminiferal oxygen isotopes in brown and IRD concentrations in pale blue. (b) New oxygen isotope record of benthic foraminiferal calcite (*C. wuellerstorfi*) in red (this study) with data of McManus et al. (1999) in brown (McManus data adjusted by -0.3‰ due to an inter-lab offset). (c) IRD concentrations, new data (this study) in dark blue ($150 - 500\ \mu\text{m}$), data from McManus et al. (1999) in pale blue (grain size $>150\ \mu\text{m}$). (d) Percentage of polar species *N. pachyderma* (s.).

as a proportion of the total number of planktonic foraminifera, with high values indicating cold sea surface temperatures (this study). (e) Oxygen isotope values of ice from NGRIP ice core, with less negative values indicating warmer temperatures (North Greenland Ice Core Project Members et al., 2004). NGRIP data plotted on the GICC05 age model (Andersen et al., 2006; Rasmussen et al., 2006; Svensson et al., 2008; Vinther et al., 2006). Grey arrows mark Site 980 recalibrated radiocarbon ages from Oppo et al. (2003) and Benway et al. (2010). Data in panels (b) – (d) are plotted on our new age model (see methods), with intervals of high ice rafting shaded in yellow.

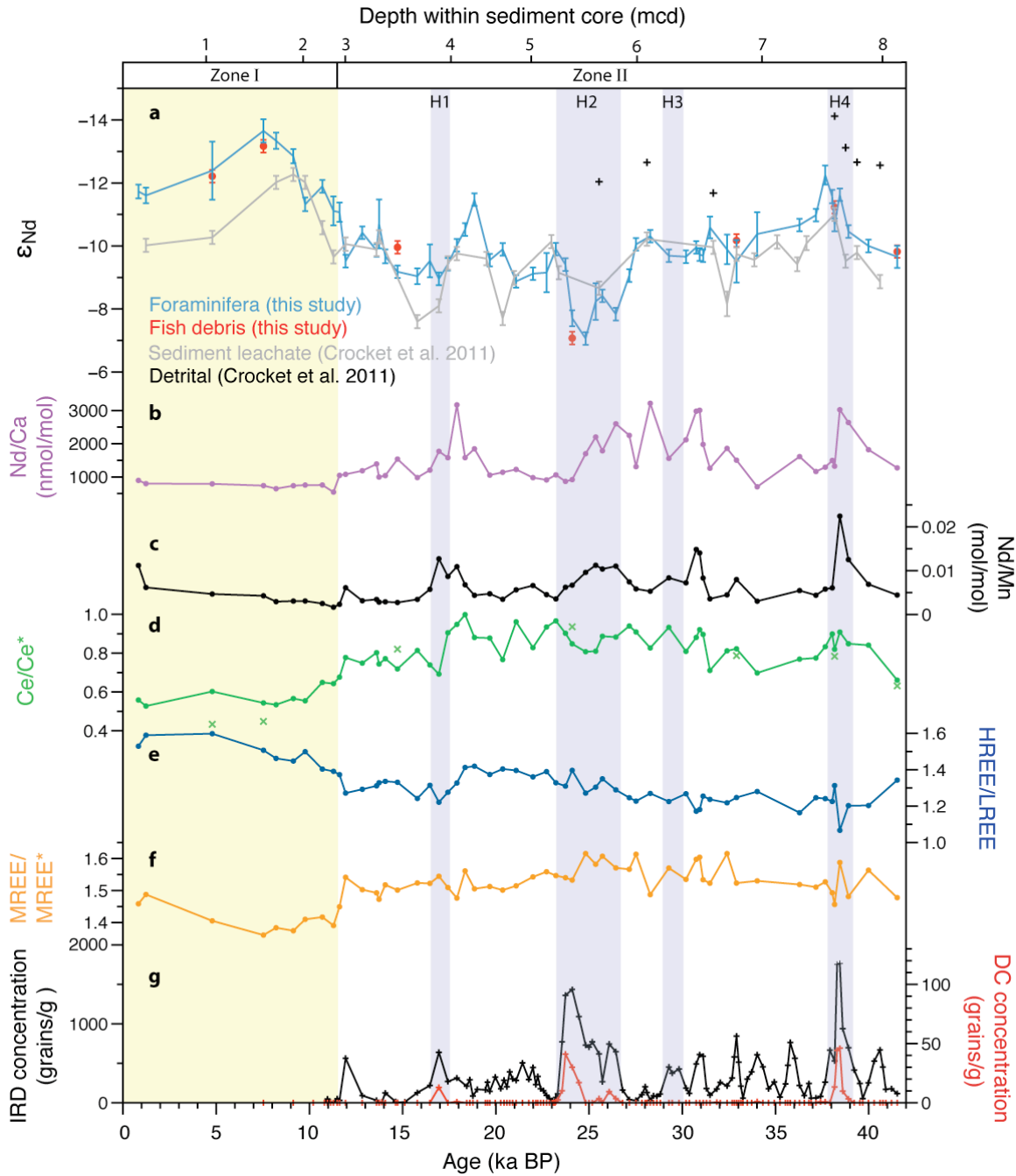


Fig. 3: ODP Site 980 neodymium isotope and rare earth element chemistry. (a) Neodymium isotope composition (and 2σ error) of mixed planktonic foraminifera (blue), fish debris (red), sediment leachates (grey, Crocket et al., 2011) and the detrital fraction (black, Crocket et al., 2011). (b) and (c) Nd/Ca and Nd/Mn ratios of mixed planktonic foraminifera. (d), (e) and (f) Ratios of mixed planktonic foraminifera PAAS-normalised REEs (X_n) with (d) $Ce/Ce^* =$

$3\text{Ce}_n/(2\text{La}_n+\text{Nd}_n)$, (e) $\text{HREE/LREE} = (\text{Er}_n+\text{Yb}_n+\text{Lu}_n)/(\text{La}_n+\text{Pr}_n+\text{Nd}_n)$, (f) $\text{MREE/MREE}^* = \text{Gd}_n+\text{Tb}_n+\text{Dy}_n/0.5(\text{La}_n+\text{Pr}_n+\text{Nd}_n+\text{Er}_n+\text{Yb}_n+\text{Lu}_n)$. Fish Ce/Ce* ratios are shown by crosses in panel (d). (g) Fluxes of ice-rafted debris (black) and detrital carbonate (red) grains from the 150 – 500 μm size fraction. Purple shading marks the timing of Heinrich-layer deposition (identified from the IRD and detrital carbonate records). Yellow shading highlights the upper section of the core in which Nd isotope ratios derived from sediment leachates are offset to more radiogenic values than the records of planktonic foraminifera and fish debris (named zone I). The deeper section of the core with higher Nd/Ca values and no systematic inter-substrate ϵ_{Nd} offset is named zone II. Note that depth within sediment core (in metres composite depth) is plotted on a non-linear scale.

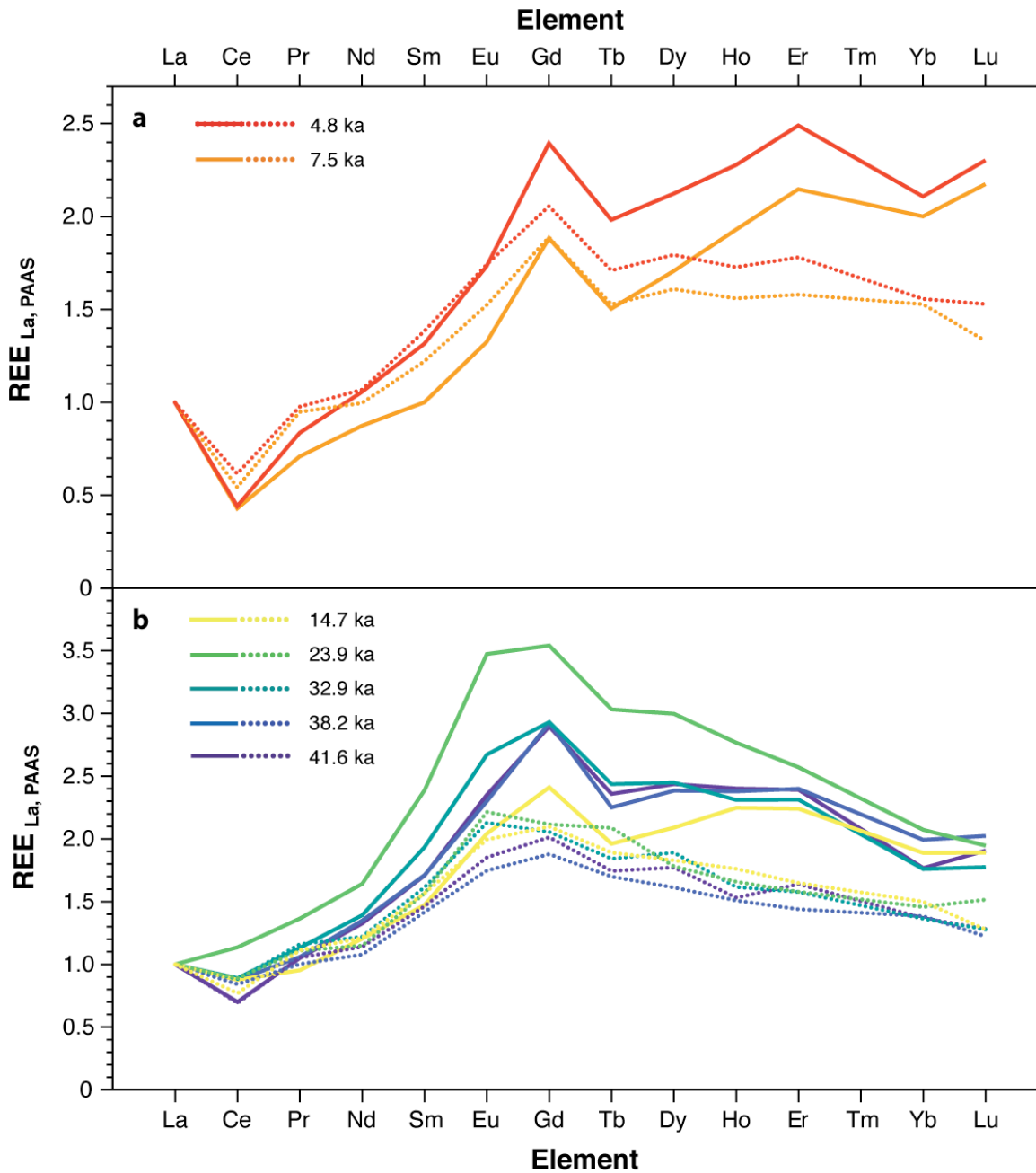


Fig. 4: Comparison of REE profiles of ODP Site 980 fish debris (dotted lines) and mixed planktonic foraminifera (solid lines). Values are normalised to PAAS and La = 1, with samples from zone I in panel (a) and zone II in panel (b). Sample ages given in figure legend.

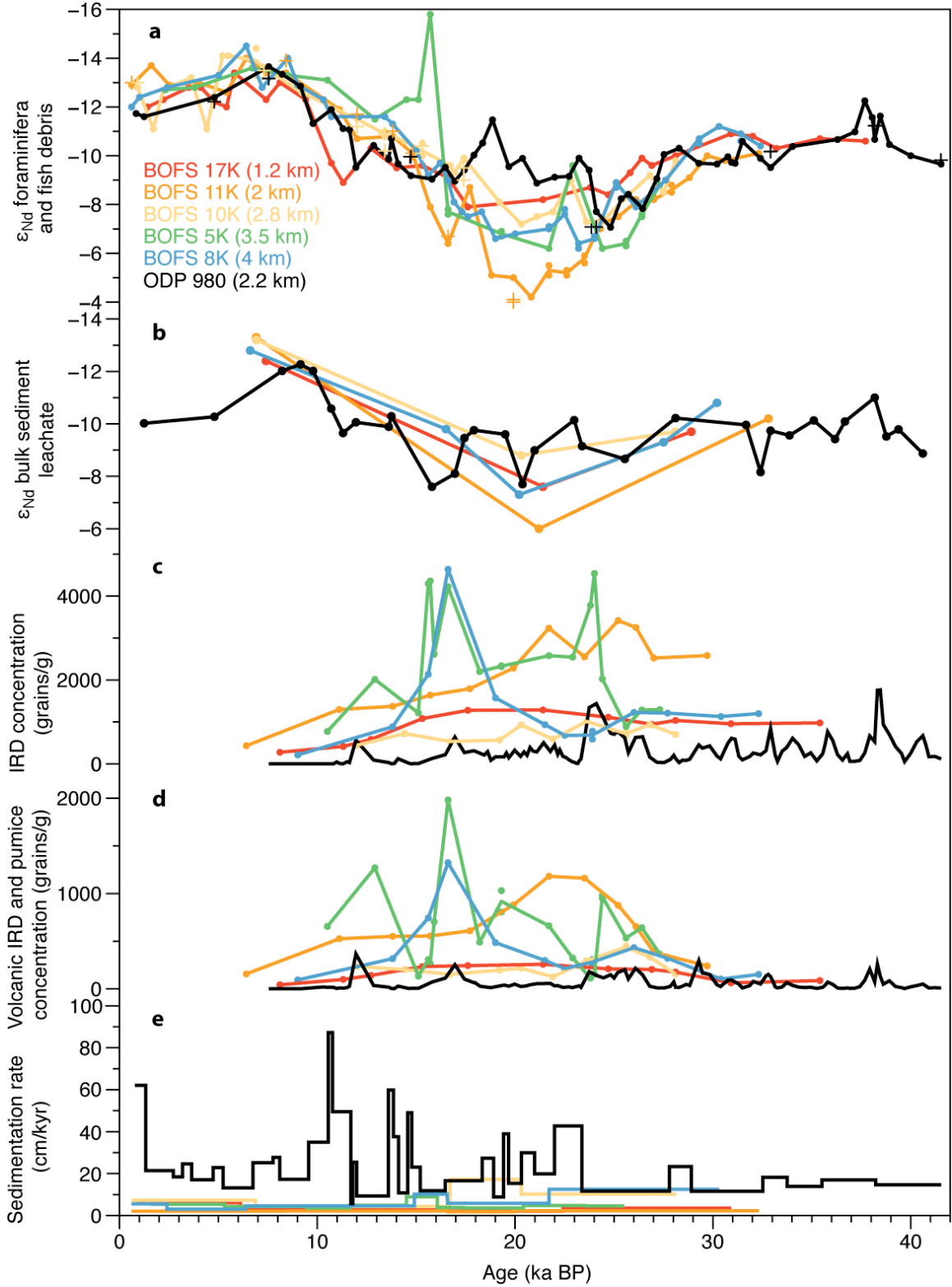


Fig. 5: Comparison of palaeoclimate records from Site 980, Feni Drift (black, this study and Crocket et al. (2011)) and BOFS sites (colour) on and along the southern flank of the Rockall

Plateau (Roberts and Piotrowski, 2015) (water depths in legend, site locations shown in Fig. 1). (a) Uncleaned foraminifera (solid circles and lines) and fish debris ϵ_{Nd} (crosses). (b) Bulk sediment leachate ϵ_{Nd} values. (c) Concentration of IRD grains 150 – 500 μm (Site 980) and >150 μm (BOFS cores (Roberts and Piotrowski, 2015)). (d) Concentration of volcanic IRD (including basalt and mafic and felsic volcanic glasses) and pumice clasts with grain size 150 – 500 μm (Site 980) and >150 μm (BOFS sites, Roberts and Piotrowski (2015)). (e) Sedimentation rates (cm/kyr) based on published age models (BOFS sites, Roberts and Piotrowski (2015)) and this study (Site 980).

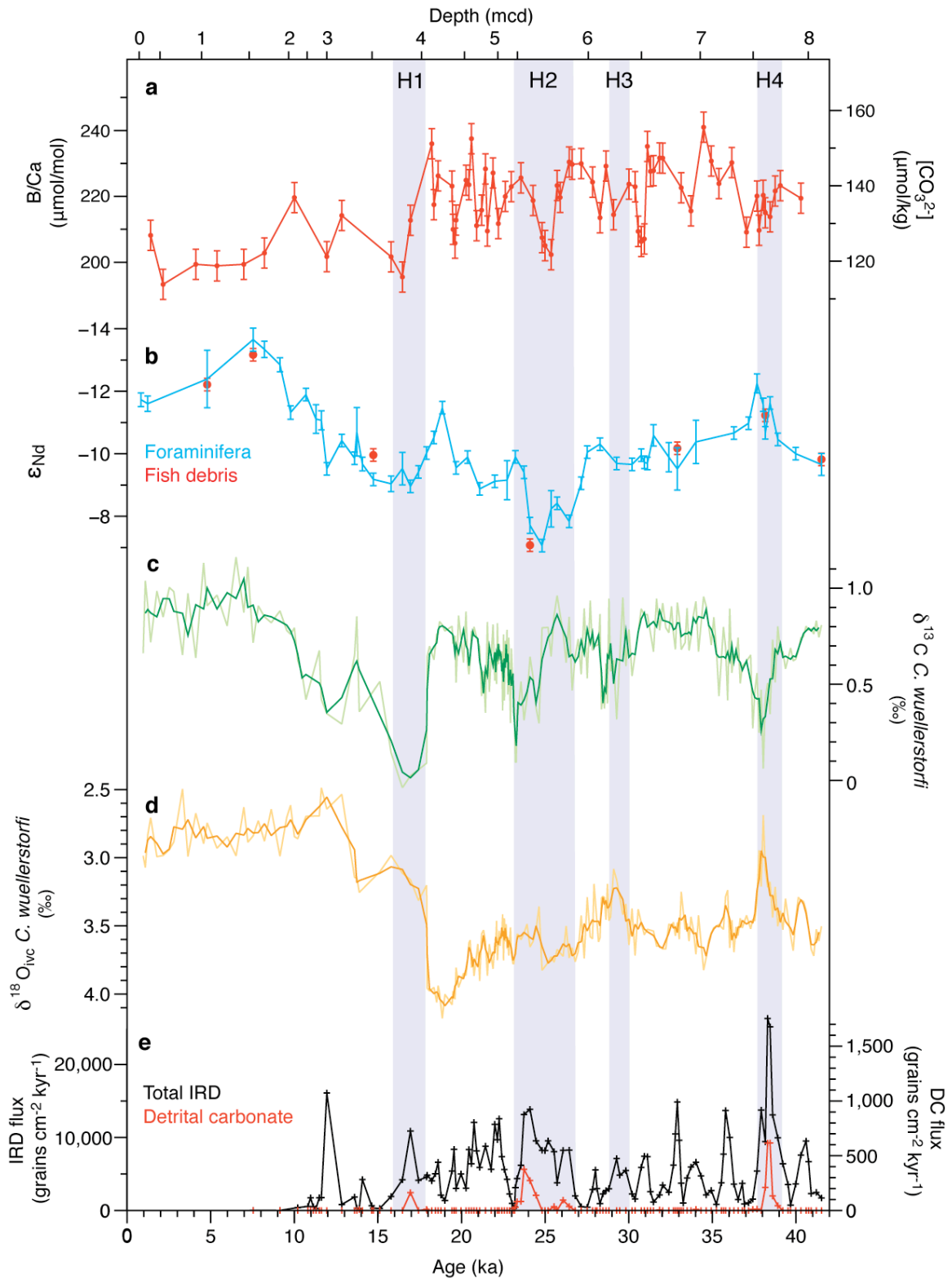


Fig. 6: Bottom water chemistry shifts at ODP Site 980 during H-events. Shaded bands mark the position of the H-events identified by IRD abundance at Site 980. (a) Bottom water carbonate ion

concentrations reconstructed from B/Ca ratios of benthic foraminifera *C. wuellerstorfi*, with error bars indicating analytical uncertainty (calibration uncertainty $\pm 10\mu\text{mol/kg}$ (Yu and Elderfield, 2007)). (b) Neodymium isotope ratios of planktonic foraminifera with ferromanganese coatings not removed (in blue) and fish debris (red) (error bars $\pm 2\sigma$). (c) $\delta^{13}\text{C}$ of *C. wuellerstorfi*, with darker line colour marking the three-point running mean. (d) $\delta^{18}\text{O}$ of *C. wuellerstorfi*, adjusted for global ice volume changes, with darker line colour marking the three-point running mean. (e) Fluxes of ice-rafted debris (black) and detrital carbonate clasts (red) in grains $150 - 500 \mu\text{m cm}^{-2} \text{ kyr}^{-1}$.

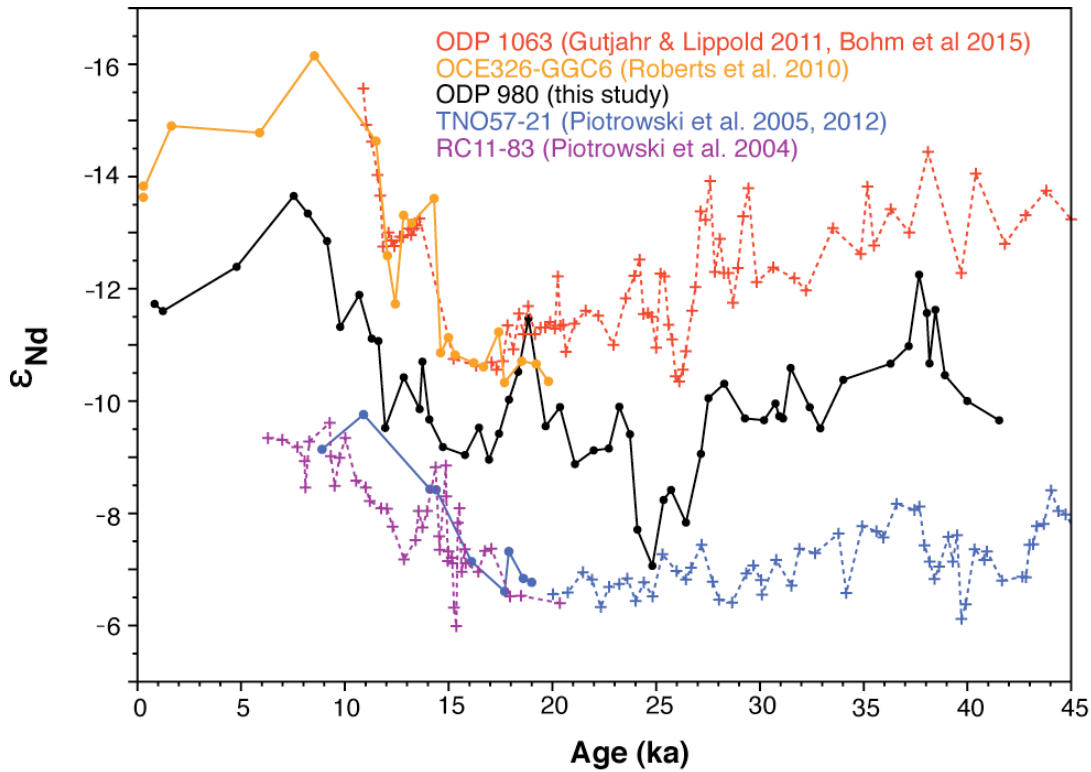


Fig. 7: Comparison of Site 980 uncleaned foraminiferal ϵ_{Nd} records (black) with deep sites at the Bermuda Rise (ODP 1063/OCE326-GGC6 in red/orange (Böhm et al., 2015; Gutjahr and Lippold, 2011; Roberts et al., 2010)) and South Atlantic (TNO57-21/RC11-83 in blue/purple (Piotrowski et al., 2012; Piotrowski et al., 2004, 2005)). Foraminiferal ϵ_{Nd} values are shown with solid lines and filled circles, while bulk sediment leachates are shown with dotted lines and crosses. Note that GGC6 bulk sediment leachate values are not shown as these were deemed not to be representative of bottom water chemistry by Roberts et al. (2010).

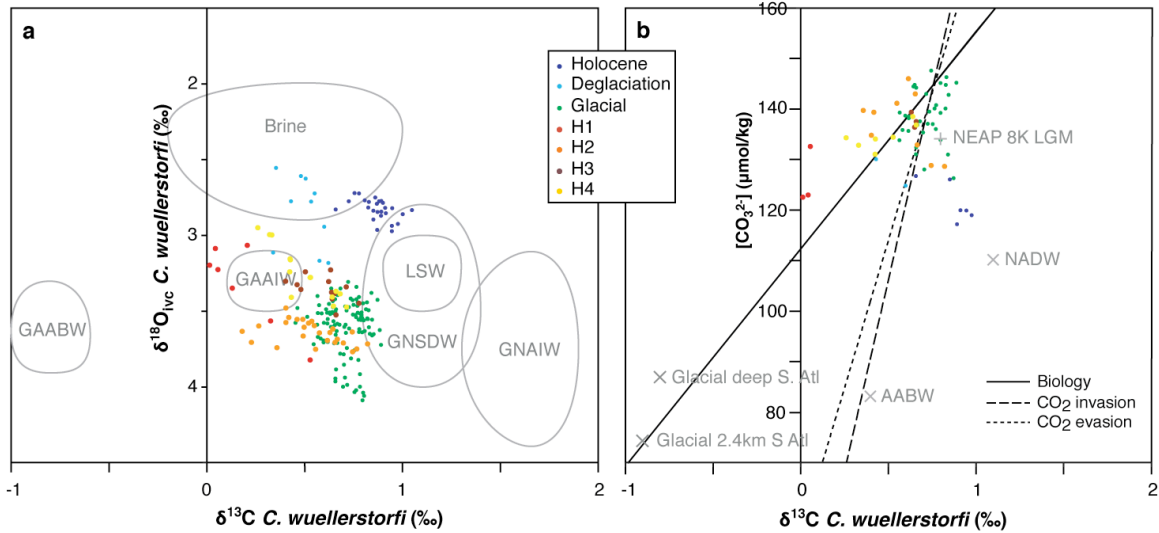


Fig. 8: Comparison of Site 980 bottom water chemistry to regional water mass signatures. (a) Cross-plot of co-measured oxygen and carbon isotopes of *C. wuellerstorfi* from ODP Site 980. All values are smoothed (3-point running mean), with $\delta^{18}\text{O}$ values adjusted for global ice volume changes. Estimated water mass compositions shown in grey, based upon Bertram et al. (1995), Voelker et al. (2006), Meland et al. (2008) and Thornalley et al. (2010). Water masses abbreviations: GAABW: Glacial Antarctic Bottom Water; GAAIW: Glacial Antarctic Intermediate Water; LSW: Labrador Sea Water (Holocene value); GNAIW: Glacial North Atlantic Intermediate Water; GNSDW: Glacial Norwegian Sea Deep Water. Note that the isotopic composition of brines has high uncertainty (e.g. Meland et al., 2008; Thornalley et al., 2010). (b) Cross-plot of $\delta^{13}\text{C} C. wuellerstorfi$ and estimated bottom water $[\text{CO}_3^{2-}]$ calculated from *C. wuellerstorfi* B/Ca ratios (see methods). Also shown are lines indicating the calculated slope of co-variance in $\delta^{13}\text{C}$ and $[\text{CO}_3^{2-}]$ generated by biological regeneration and CO_2 invasion/evasion (Yu et al., 2008). Reconstructed water mass signatures are shown in grey (data from Yu et al., 2014; Yu et al., 2008). NEAP 8K is thought to record a strong influence of overflow waters from the Nordic Seas at the Last Glacial Maximum (Yu et al., 2008).

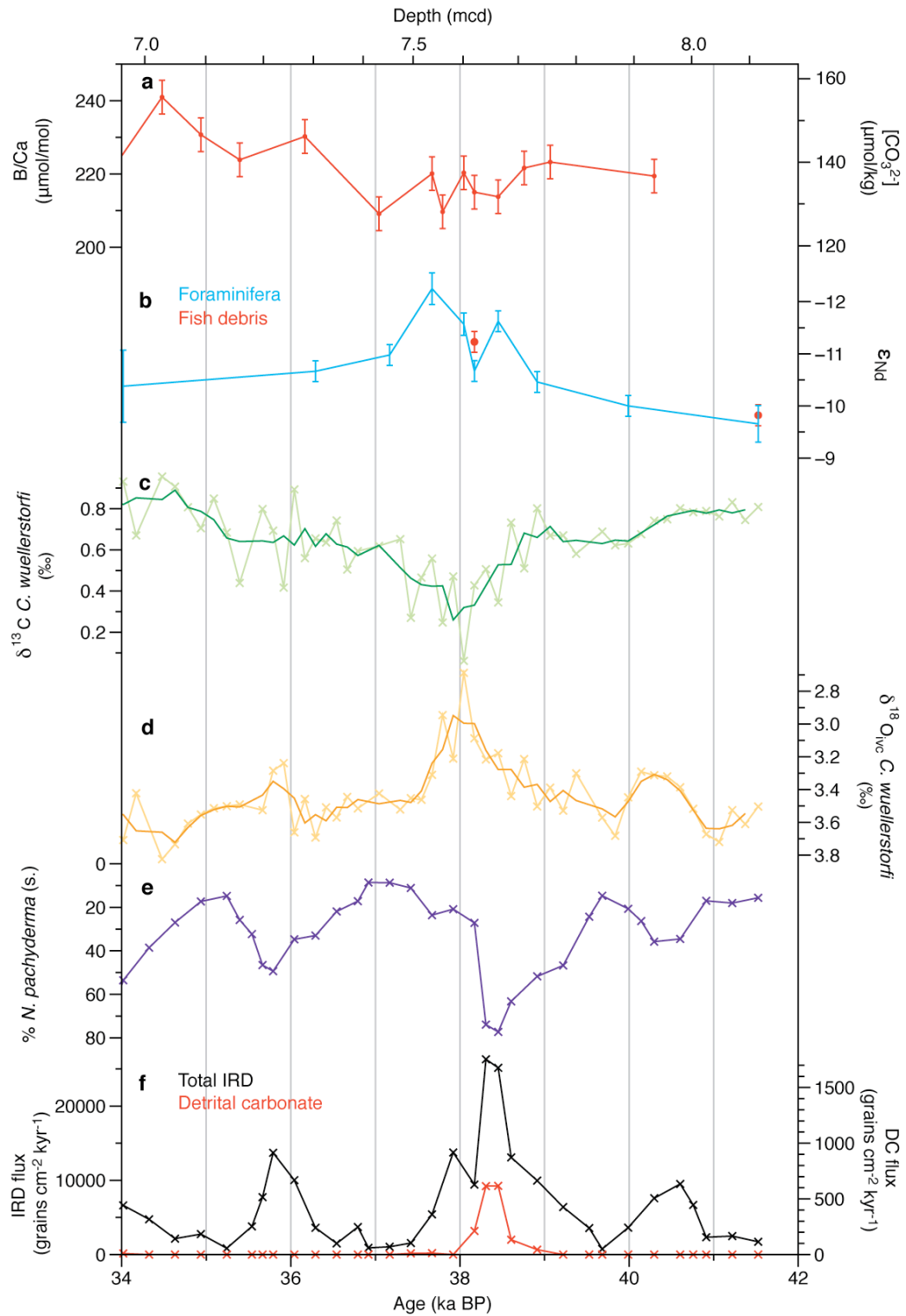


Fig. 9: Reconstruction of changes in surface and deep ocean at Site 980 during H4. (a) Bottom water carbonate ion concentrations reconstructed from B/Ca ratios of benthic foraminifera *C. wuellerstorfi* with error bars indicating analytical uncertainty (calibration uncertainty ± 10

$\mu\text{mol/kg}$ (Yu and Elderfield, 2007)). (b) Neodymium isotope ratios of planktonic foraminifera with ferromanganese coatings not removed (in blue) and fish debris (red). Error bars indicate $\pm 2\sigma$. (c) $\delta^{13}\text{C}$ of *C. wuellerstorfi*, with darker line colour marking the three-point running mean. (d) $\delta^{18}\text{O}$ of *C. wuellerstorfi*, adjusted for global ice volume changes, with darker line colour marking the three-point running mean. (e) Percentage of polar species *N. pachyderma* (s.) as a proportion of the total number of planktonic foraminifera. (f) Fluxes of ice-rafted debris (black) and detrital carbonate (red) grains from the 150 – 500 μm size fraction of Site 980 samples.

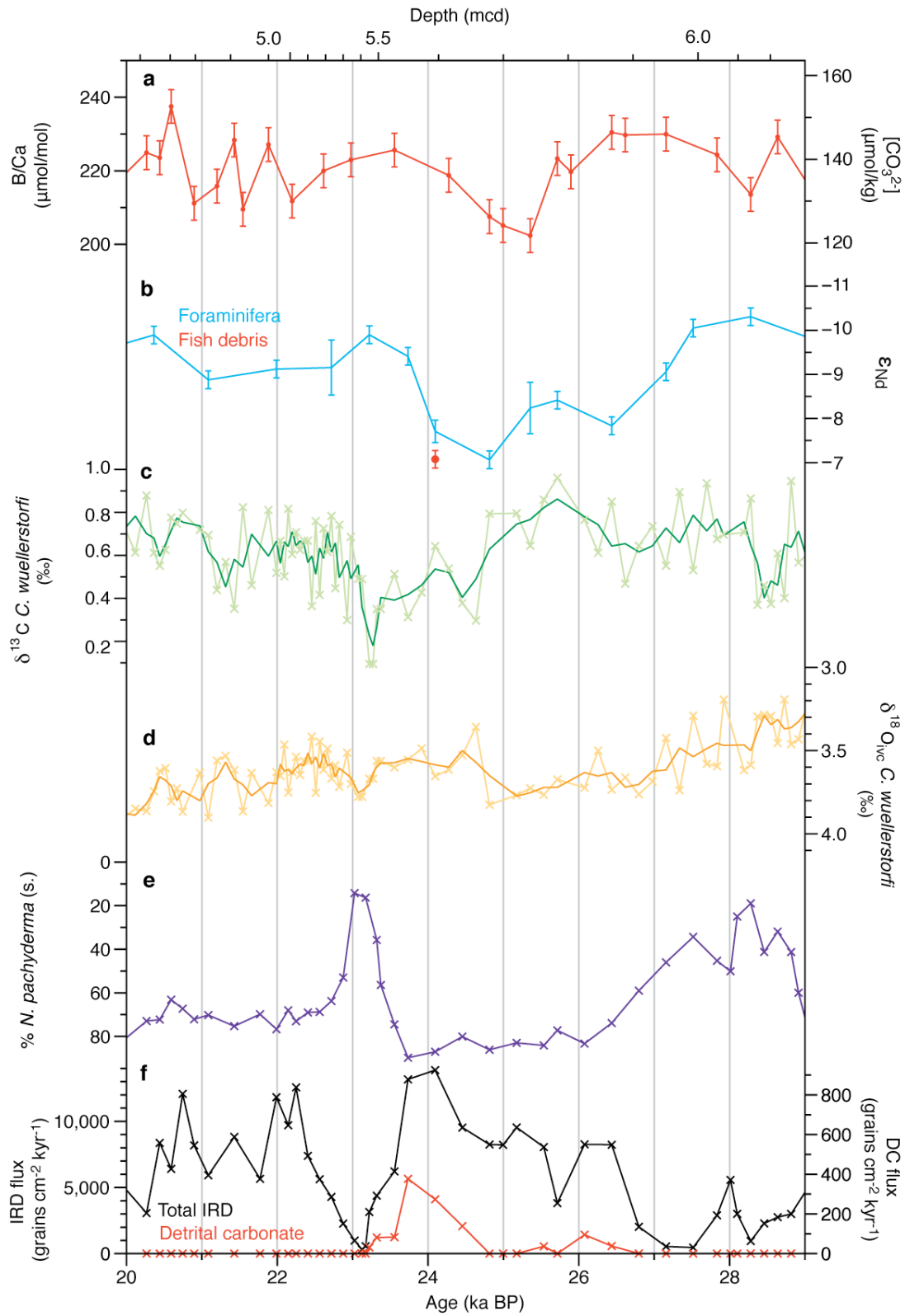


Fig. 10: Reconstruction of changes in surface and deep ocean at Site 980 during H2. Symbols as in Fig. 9.